

A new class of composite GBII regression models with varying threshold for modelling heavy-tailed data

Zhengxiao Li ^{*} Fei Wang [†] Zhengtang Zhao [‡]

Abstract

The four-parameter generalized beta distribution of the second kind (GBII) has been proposed for modelling insurance losses with heavy-tailed features. The aim of this paper is to present a parametric composite GBII regression modelling by splicing two GBII distributions using mode matching method. It is designed for simultaneous modeling of small and large claims and capturing the policyholder heterogeneity by introducing the covariates into the location parameter. The threshold that splits two GBII distributions is allowed to vary across individuals policyholders based on their risk features. The proposed regression modelling also contains a wide range of insurance loss distributions as the head and the tail respectively and provides the close-formed expressions for parameter estimation and model prediction. A simulation study is conducted to show the accuracy of the proposed estimation method and the flexibility of the regressions. Some illustrations of the applicability of the new class of distributions and regressions are provided with a Danish fire losses data set and a Chinese medical insurance claims data set, comparing with the results of competing models from the literature.

Keywords: composite GBII distribution; regression modelling; policyholder heterogeneity; varying threshold

Article History: April 19, 2022

^{*}School of Insurance and Economics, University of International Business and Economics, Beijing, China. Email: li_zhengxiao@uibe.edu.cn.

[†]School of Insurance and Economics, University of International Business and Economics, Beijing, China; Taikang Life Insurance Co.,Ltd., Beijing, China. Email: uibewangfei@163.com.

[‡]Corresponding author: ztzhaoxmu.edu.cn. Department of Finance, School of Economics, Xiamen University, Xiamen, China.

1 Introduction

For many lines of insurance business, the insurance loss data often exhibits the heterogeneity, heavy-tailedness and different tail behavior of small and large amounts. Various statistical methods have been proposed to generalized classical loss distributions to account for the above mentioned characteristics of the loss data, which are based on, but not limited to the following three methods: (1) transformation method, (2) mixed or mixture method, (3) splicing method (also known as composite model).

The transformed method provides procedures to fit the log-transformed distribution to the data with heavy-tailed features, for instance the skew Normal distribution ([Azzalini et al., 2002](#)), the log skew T distribution ([Landsman et al., 2016](#)), the generalized log Moyal distribution ([Bhati and Ravi, 2018](#)). A drawback of the transformation method is that it may magnify the error of the prediction as it changes the variance structure of the data ([Gan and Valdez, 2018](#)). The four-parameter GBII family as a transformed beta family that includes many of the classical loss distributions as a special or limiting case has been proved to be a very useful tool in the actuarial literature ([Dong and Chan, 2013](#), [Shi and Yang, 2018](#)).

Mixed or mixture model constitutes another method which deals with modeling insurance losses with unobserved heterogeneity and heavy-tailed features. This approach has been discussed in several publications in non-life actuarial literature. For example, [Chan et al. \(2018\)](#) extend the GBII family to the contaminated GBII family based on a finite mixture method which aims to capture the bimodality and a wide range of skewness and kurtosis of insurance loss data. Here, we refer to many other mixture and mixed models: a finite mixture of skew Normal distributions ([Bernardi et al., 2012](#)), a finite mixture of Erlang distributions ([Verbeelen et al., 2015](#)), a Gamma mixture with the generalized inverse Gaussian distribution ([Gómez-Déniz et al., 2013](#)), and more general finite mixture models based on the Burr, Gamma, inverse Burr, inverse Gaussian, Lognormal and Weibull distributions ([Miljkovic and Grün, 2016](#)). However, as the derivatives of the log-likelihood function of mixture models are complicated in the classical likelihood approach, the expectation-maximization (EM) techniques need to be applied in estimation procedure, which suffers significant challenges on the initialization of parameter estimates. Recently, [Punzo et al. \(2018\)](#) propose a three-parameter compound distribution (also known as mixed distribution) in order to take care of specifics such as unimodality, hump-shaped, right-skewed, and heavy tails. The resultant density obtained by this work also does not always have closed-form expressions, which makes the estimation more cumbersome.

The splicing method as the third approach provides a global model fit strategy by combining a tail fit and a distribution modelling the loss data below the threshold. Different spliced or so-called composite models emerge depending on the univariate distribution used for the head and the tail, see e.g. [Cooray and Ananda \(2005\)](#), [Scollnik \(2007\)](#), [Scollnik and Sun \(2012\)](#), [Bakar et al. \(2015\)](#) and [del Castillo et al. \(2017\)](#). In [Reynkens et al. \(2017\)](#), the modal part fit is established using a mixed Erlang distribution, which can also be adapted to censored data. This then reduces the problem of selecting a specific parametric modal part component. In [Grün and Miljkovic \(2019\)](#), a comprehensive analysis is provided for the Danish fire losses data set by evaluating 256 composite models derived from 16 parametric distributions that are commonly used in actuarial science. However, the estimation procedure in [Grün and Miljkovic \(2019\)](#) requires the numeric optimization, derivative calculation, as well as root finding methods as even the parameters in the density function does not have closed-form expressions when different combinations of distribution for the head and tail part are considered.

The use of covariate information in order to predict heavy-tailed loss data through regression models has been recently become a popular topic for insurance pricing, reserving and risk measurement as traditional generalized linear modelling such as Gamma and inverse Gaussian regression do not have specific interest in heavy-tailed modelling. An important contribution of this kind in non-life insurance rate making and reserving is [Shi and Yang \(2018\)](#) and [Dong and Chan \(2013\)](#), in which the GBII family was used as a response distribution for regression modelling. Although the regression modelling in transformed distributions and mixture/mixed distributions are well developed, for instance, the Burr regression ([Beirlant et al., 1998](#)), the generalized log-Moyal regression ([Bhati and Ravi, 2018](#)), the mixed exponential regression ([Tzougas and Karlis, 2020](#)), the subfamily of GBII regression ([Li et al., 2021](#)) and the Phase-type regression ([Bladt, 2022](#)), the use of heavy-tailed composite models in a regression setting has not been fully established yet. [Gan and Valdez \(2018\)](#) propose the use of two spliced regression models for modelling the aggregate loss data directly. The interpreting the regression coefficients of the spliced models is not straightforward. [Laudagé et al. \(2019\)](#) propose a composite model with a regression structure, only allowing the covariates to be introduced in the body of the loss distribution. While [Fung et al. \(2021\)](#) presents a mixture composite regression model by introducing systematic effects of covariates in body and tail of the distribution, the threshold is still pre-determined using export information via performing extreme value analysis. The above mentioned models also impose an additional constraint of fixed threshold when the covariates are considered, which does not reflect the policyholder heterogeneity among the tail part of the loss data. The recent work about

varying threshold used in the composite regression modelling is a deep composite regression model proposed by [Fissler et al. \(2021\)](#) whose splicing point is given in terms of a quantile of the conditional claim size distribution rather than a constant.

The aim of this paper is to introduce a general family of composite regression models with varying threshold for approximating both the modal part and the tail of heavy-tailed loss data as well as for capturing the risk heterogeneity among policyholders. For this purpose, we first splice two GBII distribution as a head and tail part respectively by using a mode-matching method proposed by [Calderín-Ojeda and Kwok \(2016\)](#). This method can incorporate unrestricted mixing weights and gives a simpler derivation of the model over the traditional continuity-differentiability method discussed in [Grün and Miljkovic \(2019\)](#). The new class of distributions contains a wide range of insurance loss distributions as the head and the tail respectively and is very flexible in modelling different shapes of distributions. It also provides the close-formed expressions for parameter estimation and model prediction. Next, the composite GBII family is used as a response distribution for regression modelling, in which the location parameter is modelled as a function of several covariates in a non-linear form. The proposed regression setting is defined so that its mean is proportional to some exponential transformation of the linear combinations of covariates. It also gives the explicit expressions of VaR and TVaR across all individuals and related to covariates when the mean does not always exist for modelling more extreme losses. Moreover, the threshold that splits the two GBII distribution varies across policyholders based on observed risk features, which allows us to capture different tail behaviors among individuals. Finally, we present a constrained maximum likelihood estimation method for estimating the unknown parameters via the augmented Lagrange multiplier method. The estimation results are demonstrated to perform satisfactorily when the composite GBII regression models are fitted to a simulation study and two real-world insurance data sets.

The structure of this paper is as follows. In Section 2 we provide a brief summary of the GBII distribution, introduce a new class of composite GBII distributions and study some properties, such as its moments and risk measure expressions. Regression modelling and estimation procedure are discussed in Section 3. The advantages of the composite GBII regressions compared to the conventional GLMs in the presence of different tail behaviors are illustrated by a simulation study in Section 4. To illustrate its practical use, in Section 5, we first fit the composite GBII models to the well-known Danish fire insurance data-set, comparing with fits based on models from existing literature. Then regression modelling is discussed with an illustration on a Chinese medical insurance data set. Section

[6](#) gives some conclusions and future possible extensions.

2 Model specifications

2.1 The GBII distribution

Let $Y \in \mathbb{R}^+$ be the insurance loss or claim amount random variable. The density of the GBII distribution is given by:

$$f_{\text{GBII}}(y; p, \mu, \nu, \tau) = \frac{|p|}{B(\nu, \tau)y} \frac{\mu^{p\tau} y^{p\nu}}{(y^p + \mu^p)^{\nu+\tau}}, \quad (2.1)$$

for $y > 0$, $\mu, \nu, \tau > 0$ with $B(m, n) = \int_0^1 t^{m-1}(1-t)^{n-1}dt$ the beta function. The GBII is a member of the log location-scale family with location parameter μ , scale parameter p , and shape parameters ν and τ ([Cummins et al., 1990](#)). When the scale parameter $p < 0$, (2.1) admit the inverse distributions, which is obtained by making the reciprocal transformation. It is easily shown that $\text{GBII}(y; -p, \mu, \tau, \nu) = \text{GBII}(y; p, \mu, \nu, \tau)$. The cdf and quantile function of the GBII distribution are given by respectively

$$F_{\text{GBII}}(y; p, \mu, \nu, \tau) = I_{\nu, \tau} \left[\frac{(y/\mu)^p}{1 + (y/\mu)^p} \right], \quad y > 0, \quad (2.2)$$

$$F_{\text{GBII}}^{-1}(q; p, \mu, \nu, \tau) = \mu \left[\frac{I_{\nu, \tau}^{-1}(q)}{1 - I_{\nu, \tau}^{-1}(q)} \right]^{\frac{1}{p}}, \quad q \in (0, 1), \quad (2.3)$$

where q is the quantile level and $I_{m, n}^{-1}(\cdot)$ denotes the inverse of the beta cumulative distribution function $I_{m, n}(\cdot)$ (or regularized incomplete beta function). The mode of the GBII occurs at

$$y_0 = \mu \left(\frac{p\nu - 1}{p\tau + 1} \right)^{1/p}, \quad \text{if } p\nu > 1, \quad (2.4)$$

and at zero otherwise.

Also, the GBII density is regularly varying at infinity with index $-p\tau - 1$ and regularly varying at the origin with index $-p\nu - 1$, which implies that all three shape parameters control the tail behavior of the distribution. The h -th moments for the GBII exist only for $-p\nu < h < p\tau$ which are given by

$$\mathbb{E}[Y^h; p, \mu, \nu, \tau] = \frac{\mu^h B(\nu + h/p, \tau - h/p)}{B(\nu, \tau)}.$$

Concerning the h -th incomplete (conditional) moments of the GBII distribution given $y \leq s$ and

$y > s$ for any positive value s , one finds

$$\mathbb{E} [Y^h; p, \mu, \nu, \tau | Y \leq s] = \mu^h \frac{B(\nu + h/p, \tau - h/p)}{B(\nu, \tau)} \frac{I_{\nu+h/p, \tau-h/p} \left[\frac{(s/\mu)^p}{1+(s/\mu)^p} \right]}{I_{\nu, \tau} \left[\frac{(s/\mu)^p}{1+(s/\mu)^p} \right]}, \quad (2.5)$$

and

$$\mathbb{E} [Y^h; p, \mu, \nu, \tau | Y > s] = \mu^h \frac{B(\nu + h/p, \tau - h/p)}{B(\nu, \tau)} \frac{1 - I_{\nu+h/p, \tau-h/p} \left[\frac{(s/\mu)^p}{1+(s/\mu)^p} \right]}{1 - I_{\nu, \tau} \left[\frac{(s/\mu)^p}{1+(s/\mu)^p} \right]}. \quad (2.6)$$

The relationship of GBII distribution with many popular distributions is summarized in Figure 1. Figure 1 shows that the special cases of GBII distribution include three-parameter distributions of log-T (LT), generalized Gamma (GG), beta distribution of the second kind (BII), Burr (B, also known as Singh-Maddala distribution) and inverse Burr (IB), GLMGA (G) and inverse GLMGA (IG) distribution ¹, the two-parameter distributions of log-Cauchy (LC), log-Normal (LN), Weibull (W), Gamma (GA), Variance Ratio (F), Lomax (L), Loglogistic (LL), Paralogistic (P) and the one-parameter distributions of half-Normal (HN), Rayleigh (R), Exponential (EXP), Chisquare (CS) and half-T (HT) distributions.

2.2 A new class of composite GBII models

Given that the GBII distribution is unimodal when the shape parameters $p\nu > 1$ and is designed to model both the light-tailed and heavy-tailed data, a new class of composite models with two GBII distributions as a head and tail fit respectively can be derived via the mode matching procedure as discussed in [Calderín-Ojeda and Kwok \(2016\)](#). This method can overcome the drawbacks of the usually used splicing method based on the continuity and differentiability condition as given e.g. in [Grün and Miljkovic \(2019\)](#) and [Bakar et al. \(2015\)](#), thus obtaining the closed-form estimates of the parameters.

The density function of composite GBII distribution that can be defined by matching two GBII

¹The GLMGA distribution is proposed by [Li et al. \(2021\)](#) by mixing a generalized log-Moyal distribution (GlogM) ([Bhati and Ravi, 2018](#)) with the gamma distribution. It is a subfamily of the GBII and belongs to the Pareto-type distribution that can be used to accommodate the extreme risks and capture both tail and modal parts of heavy-tailed insurance data. Moreover, it occupies an interesting position in between the popular GBII model and the Lomax model.

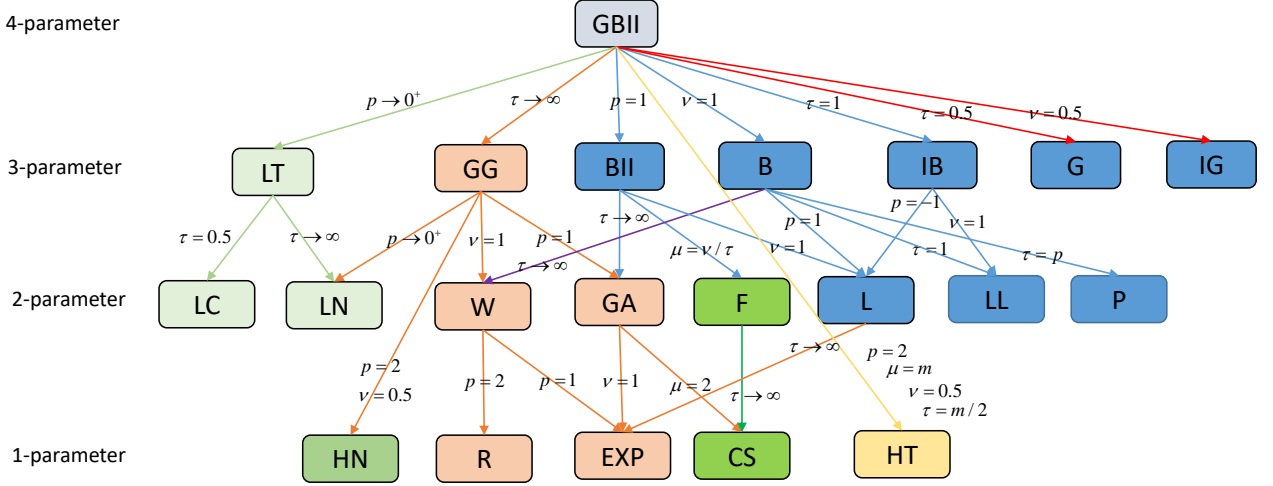


Figure 1: Family of GBII distribution.

distributions at an unknown threshold u with unfixed mixing weight r now can be written as

$$f_{\text{comGBII}}(y; \boldsymbol{\theta}) = \begin{cases} r \frac{f_{\text{GBII}}(y; p_1, \mu_1, \nu_1, \tau_1)}{F_{\text{GBII}}(u; p_1, \mu_1, \nu_1, \tau_1)}, & 0 < y \leq u \\ (1 - r) \frac{f_{\text{GBII}}(y; p_2, \mu_2, \nu_2, \tau_2)}{1 - F_{\text{GBII}}(u; p_2, \mu_2, \nu_2, \tau_2)}, & u < y < \infty \end{cases} \quad (2.7)$$

with $0 \leq r \leq 1$, $\boldsymbol{\theta} = (p_1, \mu_1, \nu_1, \tau_1, p_2, \mu_2, \nu_2, \tau_2, r, u)$ denoting the vector of parameters in the composite GBII distribution, and $p_1, \mu_1, \nu_1, \tau_1$ and $p_2, \mu_2, \nu_2, \tau_2$ denoting the vector of parameters in the head and the tail respectively.

The mode-matching procedure is used by replacing the threshold u by the modal value to satisfy the continuity and differentiability condition as the derivative at the mode is zero for unimodal distribution, yielding

$$u = y_0^1 = y_0^2, \quad (2.8)$$

$$r \frac{f_{\text{GBII}}(u; p_1, \mu_1, \nu_1, \tau_1)}{F_{\text{GBII}}(u; p_1, \mu_1, \nu_1, \tau_1)} = (1 - r) \frac{f_{\text{GBII}}(u; p_2, \mu_2, \nu_2, \tau_2)}{1 - F_{\text{GBII}}(u; p_2, \mu_2, \nu_2, \tau_2)}, \quad (2.9)$$

where y_0^1 and y_0^2 denote the mode of the distributions used by the first and the second components of

the composite model respectively. Thus, the location parameter μ_1 , the threshold (the mode) u and the mixing weight r can be calculated based on the following equations:

$$\mu_1 = \mu_2 \left[\frac{p_2\nu_2 - 1}{p_2\tau_2 + 1} \right]^{1/p_2} \left[\frac{p_1\tau_1 + 1}{p_1\nu_1 - 1} \right]^{1/p_1}, \quad (2.10)$$

$$u = \mu_1 \left[\frac{p_1\nu_1 - 1}{p_1\tau_1 + 1} \right]^{1/p_1} = \mu_2 \left[\frac{p_2\nu_2 - 1}{p_2\tau_2 + 1} \right]^{1/p_2}, \quad (2.11)$$

$$r = \frac{I_{\nu_1, \tau_1} \left[\frac{p_1\nu_1 - 1}{p_1\nu_1 + p_1\tau_1} \right]}{I_{\nu_1, \tau_1} \left[\frac{p_1\nu_1 - 1}{p_1\nu_1 + p_1\tau_1} \right] + \phi \left\{ 1 - I_{\nu_2, \tau_2} \left[\frac{p_2\nu_2 - 1}{p_2\nu_2 + p_2\tau_2} \right] \right\}}, \quad (2.12)$$

where

$$\phi = \frac{p_1}{p_2} \frac{B(\nu_2, \tau_2)}{B(\nu_1, \tau_1)} \frac{(p_2\nu_2 + p_2\tau_2)^{(\nu_2+\tau_2)}}{(p_1\nu_1 + p_1\tau_1)^{(\nu_1+\tau_1)}} \frac{(p_1\nu_1 - 1)^{\nu_1}(p_1\tau_1 + 1)^{\tau_1}}{(p_2\nu_2 - 1)^{\nu_2}(p_2\tau_2 + 1)^{\tau_2}}. \quad (2.13)$$

Note that the mixing weight r only relies on the shape parameters $(p_1, p_2, \nu_1, \nu_2, \tau_1, \tau_2)$ and the threshold u not only relies on shape parameters but also the location parameter μ_2 . It remains seven parameters $(\mu_2, p_1, p_2, \tau_1, \tau_2, \nu_1, \nu_2)$, all greater than 0, to be estimated with the two constraints $p_1\nu_1 > 1$ and $p_2\nu_2 > 1$ (the modes of the two GBII distributions must exist), while three parameters (μ_1, u, r) are implicitly determined.

The cdf of composite GBII distribution is given by

$$F_{\text{comGBII}}(y; \boldsymbol{\theta}) = \begin{cases} r \frac{F_{\text{GBII}}(y; p_1, \mu_1, \nu_1, \tau_1)}{F_{\text{GBII}}(u; p_1, \mu_1, \nu_1, \tau_1)}, & 0 < y \leq u \\ r + (1 - r) \frac{F_{\text{GBII}}(y; p_2, \mu_2, \nu_2, \tau_2) - F_{\text{GBII}}(u; p_2, \mu_2, \nu_2, \tau_2)}{1 - F_{\text{GBII}}(u; p_2, \mu_2, \nu_2, \tau_2)}, & u < y < \infty. \end{cases} \quad (2.14)$$

To show how the parameters affect the shape of the composite GBII distribution, Figure 2 plots the probability density functions when one parameter varies, keeping other parameters fixed. The thresholds are indicated by vertical dotted lines. The plots show that in all cases, that the model has positive skewness. The thresholds keep the same when the shape parameters p_1, τ_1, ν_1 in the first component varies, and vary across the values of the location and shape parameters $\mu_2, p_2, \tau_2, \nu_2$ in the second component. Also, the shape parameters τ_1, ν_1 have little effect on the density function.

The h -th moments of the composite GBII distribution exist when $-p_1\nu_1 < h < p_1\tau_1$ and $-p_2\nu_2 <$

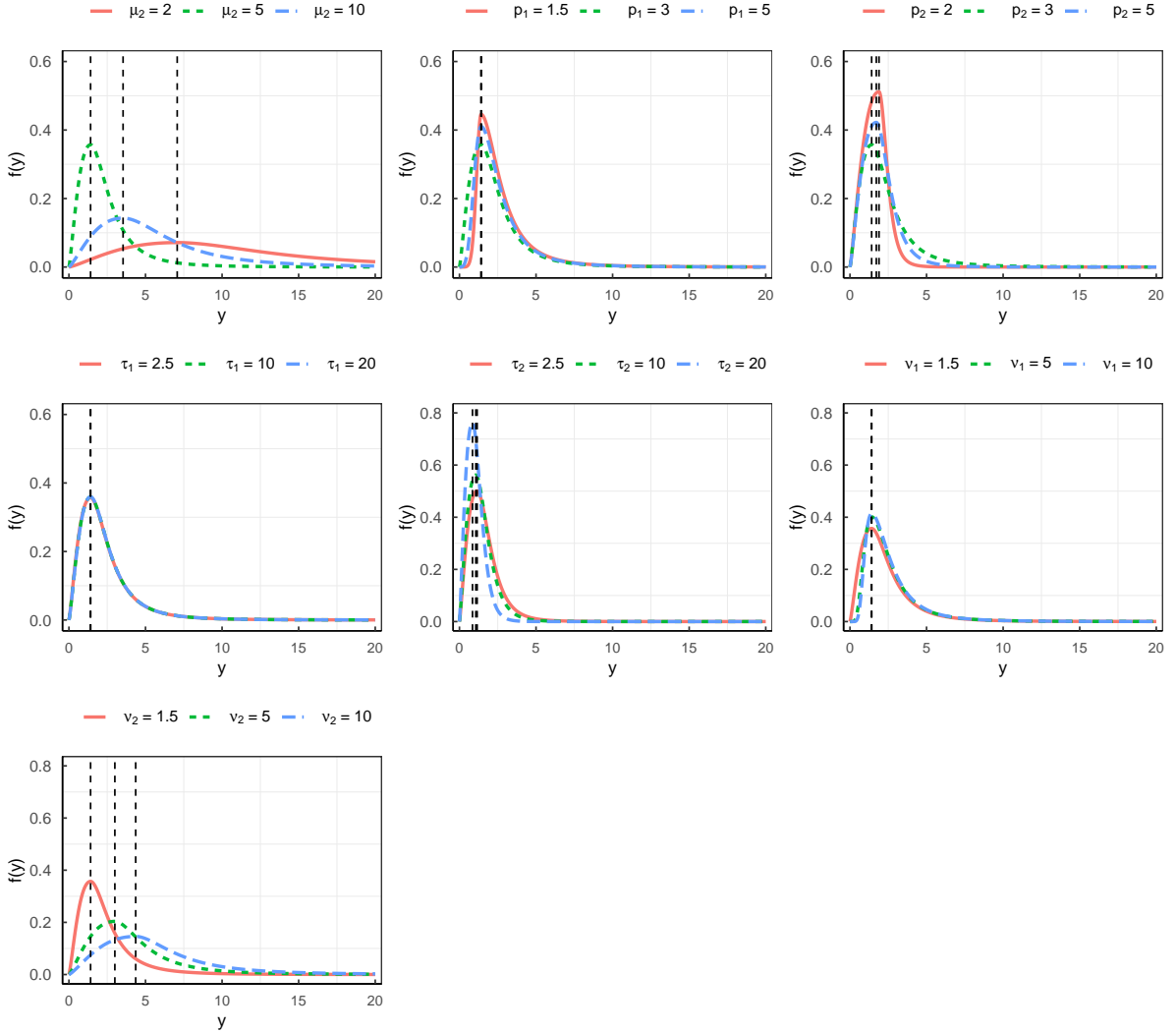


Figure 2: Density function for different composite GBII distributions when one parameter varies, keeping other parameters fixed. The default parameters are as followed: $\mu_2 = 2, p_1 = 1.5, p_2 = 2, \tau_1 = 2.5, \tau_2 = 1.5, \nu_1 = 1.5, \nu_2 = 1.5$. The thresholds are indicated by vertical dotted lines.

$h < p_2\tau_2$:

$$\begin{aligned}\mathbb{E}[Y^h; \boldsymbol{\theta}] &= r\mathbb{E}[Y^h|Y \leq u] + (1-r)\mathbb{E}[Y^h|Y > u], \\ &= r\mu_1^h \frac{B(\nu_1 + h/p_1, \tau_1 - h/p_1)}{B(\nu_1, \tau_1)} \frac{I_{\nu_1+h/p_1, \tau_1-h/p_1} \left[\frac{p_1\nu_1-1}{p_1\nu_1+p_1\tau_1} \right]}{I_{\nu_1, \tau_1} \left[\frac{p_1\nu_1-1}{p_1\nu_1+p_1\tau_1} \right]} \\ &\quad + (1-r)\mu_2^h \frac{B(\nu_2 + h/p_2, \tau_2 - h/p_2)}{B(\nu_2, \tau_2)} \frac{1 - I_{\nu_2+h/p_2, \tau_2-h/p_2} \left[\frac{p_2\nu_2-1}{p_2\nu_2+p_2\tau_2} \right]}{1 - I_{\nu_2, \tau_2} \left[\frac{p_2\nu_2-1}{p_2\nu_2+p_2\tau_2} \right]}.\end{aligned}\tag{2.15}$$

Next, a procedure for generating random variates from the composite GBII distribution is presented by using the inverse transformation method of simulation from the cdf of the two GBII distributions respectively.

- let q is generated from uniform distribution $q \sim U[0, 1]$.
- if $q \leq r$, then the random samples is generated by using the following

$$y = \mu_1 \left[\frac{I_{\nu_1, \tau_1}^{-1}(z_1)}{1 - I_{\nu_1, \tau_1}^{-1}(z_1)} \right]^{\frac{1}{p_1}}, \tag{2.16}$$

where $z_1 = qI_{\nu_1, \tau_1} \left[\frac{p_1\nu_1-1}{p_1\nu_1+p_1\tau_1} \right] / r$.

- if $q > r$, then

$$y = \mu_2 \left[\frac{I_{\nu_2, \tau_2}^{-1}(z_2)}{1 - I_{\nu_2, \tau_2}^{-1}(z_2)} \right]^{\frac{1}{p_2}}, \tag{2.17}$$

where $z_2 = F_{\text{GBII}}(u; p_2, \mu_2, \nu_2, \tau_2) + (q - r)(1 - F_{\text{GBII}}(u; p_2, \mu_2, \nu_2, \tau_2)) / (1 - r)$.

We end this section computing some important risk measure expressions for the composite GBII distribution. The Value-at-Risk (VaR) with the quantile level q was already given in (2.16) and (2.17):

$$\text{VaR}_q(Y; \boldsymbol{\theta}) = \begin{cases} \mu_1 \left[\frac{I_{\nu_1, \tau_1}^{-1}(z_1)}{1 - I_{\nu_1, \tau_1}^{-1}(z_1)} \right]^{\frac{1}{p_1}}, & q \leq r \\ \mu_2 \left[\frac{I_{\nu_2, \tau_2}^{-1}(z_2)}{1 - I_{\nu_2, \tau_2}^{-1}(z_2)} \right]^{\frac{1}{p_2}}, & q > r. \end{cases} \tag{2.18}$$

A closed-form expression for the tail Value-at-Risk (TVaR) can be obtained as in (2.6) with $s = \text{VaR}_q(Y; \boldsymbol{\theta})$ and $k = 1$:

$$\text{TVaR}_q(Y; \boldsymbol{\theta}) = \begin{cases} \mu_1 \frac{B(\nu_1 + 1/p_1, \tau_1 - 1/p_1)}{B(\nu_1, \tau_1)} \frac{1 - I_{\nu_1+1/p_1, \tau_1/p_1}(I_{\nu_1, \tau_1}^{-1}(z_1))}{1 - z_1}, & q \leq r \\ \mu_2 \frac{B(\nu_2 + 1/p_2, \tau_2 - 1/p_2)}{B(\nu_2, \tau_2)} \frac{1 - I_{\nu_2+1/p_2, \tau_2-1/p_2}(I_{\nu_2, \tau_2}^{-1}(1 - z_2))}{1 - z_2}, & q > r. \end{cases} \quad (2.19)$$

3 A composite GBII regression and statistical inference

3.1 Regression modelling

It is well known that the dependence of the response variable on the covariate(s) is modeled via the conditional mean of the response variable in generalized linear models (GLMs). However, for heavy-tailed distributions the mean may not always exist. Such distributions are extended to regression models with a link function between other model parameters such as the location, the scale or shape parameters and the covariates. [Beirlant et al. \(1998\)](#) discussed the regression modelling assuming the response variable follows the Burr distribution. [Bhati and Ravi \(2018\)](#) assumed the response variable follows the generalized log-Moyal distribution with the shape parameter being a function of the covariates. [Li et al. \(2021\)](#) constructed a new subclass models of GBII regressions. Here, we assume that the response variable Y_i follows the composite GBII distribution and propose the location parameter $\mu_2(\mathbf{x}_i; \boldsymbol{\beta})$ to be modeled as a function of the covariates \mathbf{x}_i with regression coefficients $\boldsymbol{\beta}$ for i -th observation, $i = 1, \dots, n$. In order to avoid boundary problems in optimization, we consider a log-link function obtaining real values for the location and shape parameters:

$$\begin{aligned} Y_i | \mathbf{x}_i &\sim \text{Composite GBII}(\boldsymbol{\beta}, \boldsymbol{\alpha}), \\ \log \mu_2(\mathbf{x}_i; \boldsymbol{\beta}) &= \mathbf{x}_i^T \boldsymbol{\beta}, \\ \log p_1 &= \alpha_1, \quad \log p_2 = \alpha_2, \\ \log \tau_1 &= \alpha_3, \quad \log \tau_2 = \alpha_4, \\ \log \nu_1 &= \alpha_5, \quad \log \nu_2 = \alpha_6, \end{aligned} \quad (3.1)$$

where $\boldsymbol{\alpha} = (\alpha_1, \dots, \alpha_6)$ denotes the vector of log transformation of shape parameters, $\mathbf{x}_i^T = (1, x_{i1}, \dots, x_{ik})$ denotes the vector of covariates, $\boldsymbol{\beta} = (\beta_0, \beta_1, \dots, \beta_k)^T$ the vector of coefficients.

The h -th moment of the composite GBII distribution depends on the $k + 1$ -dimensional vector of

covariates \mathbf{x}_i which is given by

$$\mathbb{E} \left[Y_i^h; \boldsymbol{\beta}, \boldsymbol{\alpha} \right] = w(\boldsymbol{\alpha}) \exp(\mathbf{x}_i^T \boldsymbol{\beta})^h, \quad (3.2)$$

where

$$\begin{aligned} w(\boldsymbol{\alpha}) := & r \frac{g_2^{1/p_2}}{g_1^{1/p_1}} \frac{B(\nu_1 + k/p_1, \tau_1 - k/p_1)}{B(\nu_1, \tau_1)} \frac{I_{\nu_1+k/p_1, \tau_1-k/p_1} \left[\frac{p_1 \nu_1 - 1}{p_1 \nu_1 + p_1 \tau_1} \right]}{I_{\nu_1, \tau_1} \left[\frac{p_1 \nu_1 - 1}{p_1 \nu_1 + p_1 \tau_1} \right]} \\ & + (1 - r) \frac{B(\nu_2 + k/p_2, \tau_2 - k/p_2)}{B(\nu_2, \tau_2)} \frac{1 - I_{\nu_2+k/p_2, \tau_2-k/p_2} \left[\frac{p_2 \nu_2 - 1}{p_2 \nu_2 + p_2 \tau_2} \right]}{1 - I_{\nu_2, \tau_2} \left[\frac{p_2 \nu_2 - 1}{p_2 \nu_2 + p_2 \tau_2} \right]}. \end{aligned}$$

Note that $w(\boldsymbol{\alpha})$ only depends on the shape parameters which are not related to covariates. Similar to the conventional GLMs, it is obvious that the mean of the composite GBII regression model are proportional to some exponential transformation of the linear predictor $\mathbf{x}_i^T \boldsymbol{\beta}$, which can provide an intuitive interpretation for the insurance pricing and reserving. Also, it provides the explicit expressions of VaR and TVaR across all individuals and related to covariates when the mean does not always exist for modelling more extreme losses. Moreover, the regression setting in (3.1) also allows a varying threshold across policyholders based on their observed risk features:

$$u(\mathbf{x}_i; \boldsymbol{\alpha}, \boldsymbol{\beta}) = \mu_2(\mathbf{x}_i; \boldsymbol{\beta}) \left[\frac{p_2 \nu_2 - 1}{p_2 \tau_2 + 1} \right]^{1/p_2}.$$

In such cases, the policyholder heterogeneity among the individuals in the tail parts of loss data can be captured sufficiently by the proposed regression model.

3.2 Constrained maximum likelihood estimation method

In this section, we will show how to perform the constrained maximum likelihood (CML) estimation method to obtain the values of the parameter vector $\boldsymbol{\beta}$ and $\boldsymbol{\alpha}$. Given a data set $\mathbf{y} = (y_1, \dots, y_n)$, the

log-likelihood function of the proposed composite GBII regression is given by

$$\begin{aligned}\ell(\boldsymbol{\beta}, \boldsymbol{\alpha}; \mathbf{y}) = & \sum_{i=1}^n \log [r(\boldsymbol{\alpha})] I[y_i \leq u(\mathbf{x}_i; \boldsymbol{\beta})] + \sum_{i=1}^n \log f_{\text{GBII}}(y_i; \mu_1(\mathbf{x}_i; \boldsymbol{\beta}), p_1, \nu_1, \tau_1) I[y_i \leq u(\mathbf{x}_i; \boldsymbol{\beta})] \\ & - \sum_{i=1}^n \log I_{\nu_1, \tau_1} \left[\frac{p_1 \nu_1 - 1}{p_1 \nu_1 + p_1 \tau_1} \right] I[y_i \leq u(\mathbf{x}_i; \boldsymbol{\beta})] \\ & + \sum_{i=1}^n \log [1 - r(\boldsymbol{\alpha})] I[y_i > u(\mathbf{x}_i; \boldsymbol{\beta})] + \sum_{i=1}^n \log f_{\text{GBII}}(y_i; \mu_2(\mathbf{x}_i; \boldsymbol{\beta}), p_2, \nu_2, \tau_2) I[y_i > u(\mathbf{x}_i; \boldsymbol{\beta})] \\ & - \sum_{i=1}^n \log \left\{ 1 - I_{\nu_2, \tau_2} \left[\frac{p_2 \nu_2 - 1}{p_2 \nu_2 + p_2 \tau_2} \right] \right\} I[y_i > u(\mathbf{x}_i; \boldsymbol{\beta})].\end{aligned}$$

Note that CML estimation can be accomplished relatively easily subjected to $p_1 \nu_1 > 1$ and $p_2 \nu_2 > 1$ by solving the following nonlinear programming problem:

$$\max_{\boldsymbol{\beta}, \boldsymbol{\alpha} \in \mathbb{R}^{k+7}} \ell(\boldsymbol{\beta}, \boldsymbol{\alpha}; \mathbf{y}) \quad (3.3)$$

$$\text{s.t. } h_1(\boldsymbol{\alpha}) = \epsilon_1 - (\alpha_1 + \alpha_5) \leq 0 \quad \text{and} \quad h_2(\boldsymbol{\alpha}) = \epsilon_2 - (\alpha_2 + \alpha_6) \leq 0, \quad (3.4)$$

where k is the number of covariates, ϵ_1 and ϵ_2 denote the small enough values with positive support, e.g., $\epsilon_1 = \epsilon_2 = 10e^{-6}$. The values of the parameter vector $\boldsymbol{\beta}$ and $\boldsymbol{\alpha}$ can be obtained using augmented Lagrange multiplier method (see e.g. Nocedal and Wright (2006)) which is a class of algorithms for constrained nonlinear optimization that enjoy favorable theoretical properties for finding local solutions from arbitrary starting points. Thus, the objective function for the inequality constrained problem (3.3)-(3.4) is given by

$$L_\rho(\boldsymbol{\beta}, \boldsymbol{\alpha}, \boldsymbol{\lambda}) := -\ell(\boldsymbol{\beta}, \boldsymbol{\alpha}; \mathbf{y}) + \sum_{k=1}^2 \lambda_k h_k(\boldsymbol{\alpha}) + \sum_{k=1}^2 \frac{\rho}{2} [\max(0, h_k(\boldsymbol{\alpha}))^2],$$

where $\boldsymbol{\lambda} = (\lambda_1, \lambda_2) \in \mathbb{R}_+^2$ are the Lagrange multipliers and $\rho > 0$ is a penalty parameter. Algorithm 1 gives the details of the augmented Lagrange multiplier method for CML estimation. The gradients of the log-likelihood function $\ell(\boldsymbol{\beta}, \boldsymbol{\alpha}; \mathbf{y})$ are needed in this step, which are given in Appendix A. The asymptotic variance-covariance matrix can be computed as the inverse of the observed Fisher information matrix, which can be obtained using the second-order derivatives of the log-likelihood function $\ell(\boldsymbol{\beta}, \boldsymbol{\alpha}; \mathbf{y})$. The estimation results are obtained using sequential quadratic programming (SQP) optimization via function `solnp` as part of the package **Rsolnp** in R software. For additional

information regarding this optimization procedure, we refer the reader to [Ye \(1987\)](#) and [Gill et al. \(2005\)](#).

Algorithm 1: augmented Lagrange multiplier method for composite GBII regression

Data: positive data points $\mathbf{y} = (y_1, \dots, y_n)$, covariates $\mathbf{x}_1, \dots, \mathbf{x}_n$, and initial parameters $\boldsymbol{\beta}^{(0)}$ and $\boldsymbol{\alpha}^{(0)}$, Lagrange multiplier vector $\boldsymbol{\lambda}^{(0)}$, penalty parameter $\rho^{(0)}$, increment c , tolerance ϵ ;

Result: CML estimations $\boldsymbol{\beta}^*$, $\boldsymbol{\alpha}^*$ and $\boldsymbol{\lambda}^*$;

set $t = 0$;

while $\|\nabla_{\boldsymbol{\beta}, \boldsymbol{\alpha}} L_{\rho^{(t)}}(\boldsymbol{\beta}^{(t)}, \boldsymbol{\alpha}^{(t)}, \boldsymbol{\lambda}^{(t)})\| \geq \epsilon$ **do**

solve for $\boldsymbol{\beta}^{(t+1)} = \arg \min_{\boldsymbol{\beta}} L_{\rho^{(t)}}(\boldsymbol{\beta}^{(t)}, \boldsymbol{\alpha}^{(t)}, \boldsymbol{\lambda}^{(t)})$;

solve for $\boldsymbol{\alpha}^{(t+1)} = \arg \min_{\boldsymbol{\alpha}} L_{\rho^{(t)}}(\boldsymbol{\beta}^{(t)}, \boldsymbol{\alpha}^{(t)}, \boldsymbol{\lambda}^{(t)})$;

update the Lagrange multipliers: $\lambda_j^{(t+1)} = \lambda_j^{(t)} + 2\rho^{(t)} h_j(\boldsymbol{\alpha}^{*(t)})$, $j = 1, 2$;

set $\rho^{(t+1)} = c\rho^{(t)}$ and $t = t + 1$;

end

3.3 Model selection

To compare models with the different number of parameters, in terms of goodness-of-fit, we consider the Akaike information criterion (AIC; [Akaike, 1974](#)) and the Bayesian information criterion (BIC; [Schwarz, 1978](#)), defined respectively as

$$\text{AIC} = -2\ell(\boldsymbol{\beta}, \boldsymbol{\alpha}; \mathbf{y}) + 2m,$$

$$\text{BIC} = -2\ell(\boldsymbol{\beta}, \boldsymbol{\alpha}; \mathbf{y}) + m \log n,$$

where ℓ denotes the log-likelihood value, m the number of model parameters and n the number of observations. The BIC gives more penalties than AIC does. The model with the minimum AIC or BIC value is selected as the preferred model to fit the data whereas the BIC gives more penalties than AIC.

For assessment of the regression model we also use randomized quantile residuals defined by $r_i = \Phi^{-1} [F_{\text{comGBII}}(y_i; \hat{\boldsymbol{\beta}}, \hat{\boldsymbol{\alpha}})]$ ($i = 1, \dots, n$), where $\Phi(\cdot)$ is the cdf of the standard normal distribution and F_{comGBII} denotes the cdf of the composite GBII model as given in (2.14). The distribution of r_i converges to standard normal if $(\hat{\boldsymbol{\beta}}, \hat{\boldsymbol{\alpha}})$ are consistently estimated, see [Dunn and Smyth \(1996\)](#), and hence a normal QQ-plot of the r_i should follow the 45 degree line for the regression application to be relevant.

4 Simulation study

In this section, we first check the accuracy of the CML estimators discussed in Section 3, and then evaluate the performance of the proposed model, compared with the conventional GLMs in the case that the tail behavior of the simulated loss data is explained by several observed covariates which characterize the individuals.

We generated $N = 1000$ data sets of sample size $n = 2000$ from the composite GBII model with $k = 2$, $\beta = (2, 0.5, 0.2)$, $\alpha = (\log(1.5), \log(1), \log(2), \log(1.5), \log(2), \log(1.5))$, $\mathbf{x}_i^T = (1, x_{i1}, x_{i2})$ and the covariates x_{i1} and x_{i2} being generated from the standard normal distribution. The parameters of the composite GBII regression are obtained using exponential transformation, that is, $\mu_2(\mathbf{x}_i) = \exp(2 + 0.5x_{i1} + 0.2x_{i2})$, $p_1 = 1.5$, $p_2 = 1$, $\tau_1 = 2$, $\tau_2 = 1.5$, $\nu_1 = 2$ and $\nu_2 = 1.5$. The maximum likelihood estimates for each simulation are calculated by using CML method. In Figure 3, we present the boxplots of the parameter estimates β from 1000 Monte Carlo simulations. The median estimate of β_0 is 2.00, while the mean is with maximum 2.52 and minimum -6.80 and 5.80% of the 1000 sample estimates is situated below the lower limit of this figure. The estimates of β_1 and β_2 are very close to the true values with small variation. Moreover, the median estimates of $\alpha_1, \alpha_2, \alpha_4$ and α_6 are very close to the true values, while the estimates of α_3 and α_5 show more bias. Note that 14.6% and 6.7% of the 1000 sample estimates of α_3 and α_5 lie out of the range of the figure limit.

To further investigate the global fitting performance of the proposed composite GBII regression model when both the body and the tail behavior of the loss data vary across individuals that are related to several covariates, we simulate the $n = 2000$ samples from the following steps:

- The covariates x_{i1} and x_{i2} are generated from the standard normal distribution for $i = 1, \dots, 2000$, and consider the loss data being simulated from two components: the body and the tail part respectively. The covariates both have effects on small and large amounts.
- The loss data in the first component is generated from a Gamma distribution with the mean parameter $\mu_{GA} = \exp(2 + 2x_{i1} + 1.5x_{i2})$, the dispersion parameter $\phi_{GA} = 1.5$, which is denoted by $Y_i \sim GA(\mu_{GA}(\mathbf{x}_i), \phi_{GA})$ for $i = 1, \dots, 1800$.
- The loss data in the second component is generated from a generalized Pareto distribution (GPD) with the location parameter $\mu_{GPD} = \exp(1 + 0.5x_{i1} + 0.5x_{i2})$, the scale parameter $\sigma_{GPD} = \exp(3 + 0.5x_{i1} + x_{i2})$ and the shape parameter $\xi_{GPD} = 1.5$, which is denoted by

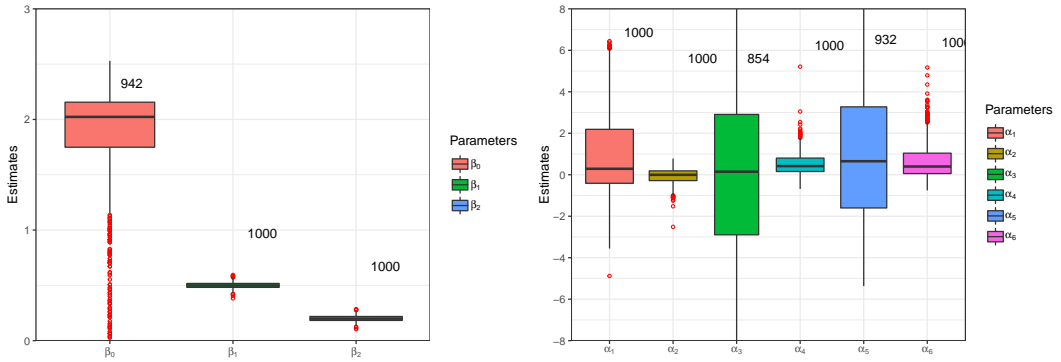


Figure 3: Boxplots of the parameter estimates from 1000 composite GBII simulated samples of size $n = 2000$. *Left:* results for the regression coefficients β_0, β_1 and β_2 . *Right:* results for the log-transformation of shape parameters $\alpha_1, \alpha_2, \alpha_3, \alpha_4, \alpha_5, \alpha_6$. The number of included samples are given next to each boxplot.

$Y_i \sim \text{GPD}(\mu_{\text{GPD}}(\mathbf{x}_i), \sigma_{\text{GPD}}(\mathbf{x}_i), \xi_{\text{GPD}})$ for $i = 1801, \dots, 2000$. Note that the location parameter in the GPD is regarded as the threshold that is modelled as a function of individual risk features in this regression setting.

We now fit the proposed composite GBII model and two GLMs, i.e., Gamma regression and inverse Gaussian regression to this simulated data set. The estimation results as well as negative log-likelihood values (NLL), the Akaike Information Criterion (AIC) and the Bayesian Information Criterion (BIC) values are reported in Table 1. The AIC and BIC select the overall best model to be the composite GBII model. Figure 4 presents the normal QQ-plots of quantile residuals from three fitted models in one Monte Carlo simulation. In terms of goodness-of-fit, we visually confirm from this figure that the distributional features of the data are perfectly captured by the proposed regression model as the varying threshold allows us to model the different tail behaviors for all individuals related to their observed risk features.

Table 1: Simulated data set: estimation results of composite GBII regression model and two GLMs.

Parameters	Composite GBII		GA		IG	
	Estimates	S.E.	Estimates	S.E.	Estimates	S.E.
Intercept	-4.56	1.53	5.30	0.03	5.26	0.78
β_1	1.41	0.04	0.50	0.03	0.46	0.60
β_2	1.14	0.03	0.69	0.03	0.59	0.56
NLL	-17598.03		-18857.99		-23976.59	
AIC	35214.06		37723.98		47961.18	
BIC	35269.76		37748.74		47985.93	

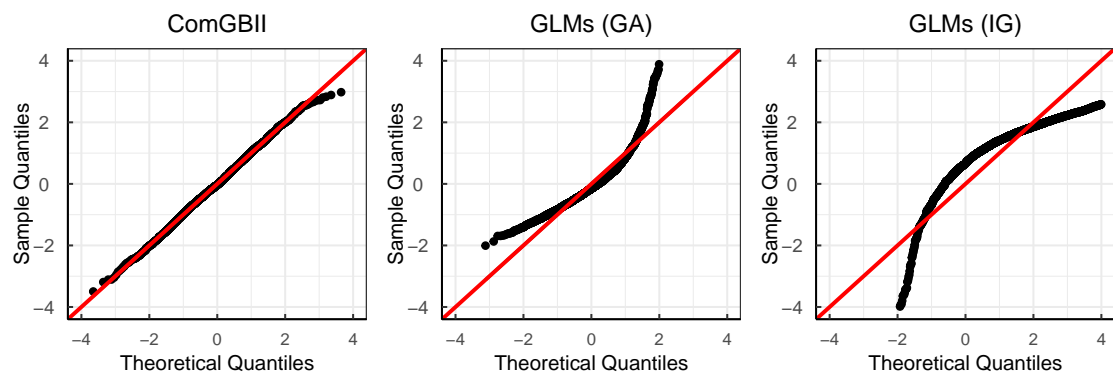


Figure 4: Normal QQ-plots of quantile residuals from the composite GBII regression and two GLMs (GA and IG) in one Monte Carlo simulations with sample size $n = 2000$.

5 Applications

In this section, we will illustrate the proposed method with the two practical examples. The first example concerns modelling the univariate loss data set without covariates by considering well-known danish fire insurance data. The second example is about investigating the behavior of the proposed regression model with covariates for modelling the short-term medical insurance claim data from a Chinese insurance company.

5.1 Danish fire insurance data set

As the first example, we fit the univariate composite GBII distribution and its subfamilies to the well-known danish fire insurance data. The data set contains of $n = 2492$ fire losses, in millions of Danish Krone (DKK) for the period 1980-1990 inclusively, and have been adjusted to reflect to inflation. The following reports some summary statistics for the data: minimum is 0.3134, 25% quantile is 1.1570, 0.75% quantile is 2.6450, maximum is 263.3, mean is 3.0630, and standard deviation is 7.9767. This data set is available in the R package **SMPPracticals**, which was also studied in [Cooray and Ananda \(2005\)](#), [Scollnik \(2007\)](#), [Calderín-Ojeda and Kwok \(2016\)](#), [Scollnik and Sun \(2012\)](#), [Bakar et al. \(2015\)](#), [Nadarajah and Bakar \(2014\)](#), and [Grün and Miljkovic \(2019\)](#) using a variety of composite models.

We now specify several composite GBII models paying special attention to the subfamily of GBII distribution. Several loss distributions that the GBII nests as special cases are considered ([Klugman et al. \(2012\)](#); p.669-681):

- the three-parameter Burr (Singh-Maddala distribution) and inverse Burr are obtained for $\nu = 1$ and $\tau = 1$ respectively.
- the three-parameter Beta distribution of the second kind is obtained for $p = 1$.
- the three-parameter GLMGA is obtained for $\nu = \frac{1}{2}$.
- the two-parameter Paralogistic and inverse Paralogistic are obtained for $\tau = p, \nu = 1$ and $\tau = 1, \nu = p$ respectively.

The details of distributions nested within the GBII distribution are shown in Appendix B. The composite models we considered are restricted to those with a three-parameter GLMGA (G) distribution forming the tail and the head belonging to the GBII and its subfamily consisting of two or

three parameters: the GBII, the Beta distribution of the second kind (BII), the Burr (B), the inverse Burr (IB), the Paralogistic (P) and the inverse Paralogistic (IP). Thus, the seven composite models are given as follows:

- Composite GBII model (ComGBII) $(p_1, \nu_1, \tau_1, \mu_2, p_2, \nu_2, \tau_2)$.
- GBIIG model $(p_1, \nu_1, \tau_1, \mu_2, p_2, \nu_2 = \frac{1}{2}, \tau_2)$.
- BIIG model $(p_1 = 1, \nu_1, \tau_1, \mu_2, p_2, \nu_2 = \frac{1}{2}, \tau_2)$.
- BG model $(p_1, \nu_1 = 1, \tau_1, \mu_2, p_2, \nu_2 = \frac{1}{2}, \tau_2)$.
- IBG model $(p_1, \nu_1, \tau_1 = 1, \mu_2, p_2, \nu_2 = \frac{1}{2}, \tau_2)$.
- PG model $(p_1, \nu_1 = 1, \tau_1 = p_1, \mu_2, p_2, \nu_2 = \frac{1}{2}, \tau_2)$.
- IPG model $(p_1, \nu_1 = p_1, \tau_1 = 1, \mu_2, p_2, \nu_2 = \frac{1}{2}, \tau_2)$.

In Table 2 we provide the estimates and standard errors of the seven models above. The method of constrained maximum likelihood was used and the standard errors were computed by inverting the observed information matrix. Table 3 reports negative log-likelihood values (NLL), as well as the Akaike Information Criterion (AIC) and the Bayesian Information Criterion (BIC) values of the proposed models. The results of six composite models discussed in [Grün and Miljkovic \(2019\)](#) are also reported in Table 3 for model comparison. It is clear from Table 3 that the BG model provides a best fit, as it has the smallest AIC and BIC values, followed by the GBIIG (according to AIC) and PG model (according to BIC) . While WIW, PIW and IBW in [Grün and Miljkovic \(2019\)](#) rank the third to fifth position based on BIC with the Inverse Weibull being in the tail part, there is not much difference between these three models as the BIC values are very close.

The goodness-of-fit measures and the bootstrap P-values for the corresponding goodness-of-fit tests of all the competing models are reported in Table 4. We consider the Kolmogorov-Smirnov (KS), Anderson-Darling (AD) and Cramér-von Mises (CvM) test statistics with corresponding P-values, choosing for the models with small values of the KS, AD and CvM test statistics, or large values of the corresponding P-values. The P-values are obtained using the bootstrap method as developed in [Calderín-Ojeda and Kwok \(2016\)](#). Here again the proposed seven models are prevailing with a P-value above 0.6, which all shows the better fit than the competing models.

Table 2: Danish fire insurance claims: model estimation

Models	ComGBII	GBIIG	BIIG	BG	IBG	PG	IPG
μ_2	1.17 (2.36)	1.03 (1.79)	1.04 (1.48)	1.03 (1.45)	1.03 (1.79)	1.03 (1.47)	1.04 (2.34)
p_1	709.11 (1264.2)	540.44 (764.97)	1 (-)	16.19 (22.95)	137.18 (194.87)	16.27 (23.1)	5.03 (7.04)
p_2	5.84 (0.67)	4.55 (0.16)	6.52 (9.52)	5.12 (0.16)	4.69 (0.14)	5.13 (0.17)	7.46 (0.17)
τ_1	7×10^6 (7×10^5)	0.59 (0.28)	12859.23 (701.93)	1146.7 (86.92)	1 (-)	16.27 (23.1)	1 (-)
τ_2	0.24 (0.12)	0.32 (0.02)	0.22 (0.07)	0.28 (0.02)	0.30 (0.42)	0.28 (0.02)	0.19 (0.01)
ν_1	0.02 (4.33)	0.03 (0.04)	43.72 (76.44)	1 (-)	0.11 (0.01)	1 (-)	5.03 (7.04)
ν_2	0.26 (0.76)	0.5 (0.13)	0.5 (-)	0.5 (-)	0.5 (-)	0.5 (-)	0.5 (-)

* The standard errors of estimates are reported in parentheses.

* The standard errors for the location and shape parameters in composite GBII models are calculated by using delta method.

In Figure 5, the QQ-plots of the empirical quantiles against the estimated quantiles of quantile residuals from the seven proposed models are given. The correlation coefficients R of these QQ-plots are also given in Table 4: R measures the degree of linearity in the QQ-plot and hence also the goodness-of-fit with respect to the corresponding model. One can see that the plots in Figure 5 also indicate that the proposed seven distributions all give good fits in the sense that the points corresponding to the theoretical and empirical quantiles do not deviate much from the 45° straight line.

Finally, Table 5 reports the empirical and estimated values of the VaR and TVaR at confidence levels of 95% and 99%. The percentage of variation of each estimated VaR and TVaR, with respect to the empirical VaR and TVaR, is also reported. In the VaR case, when the 95% confidence level is considered, the best model is IPG, which slightly underestimates the empirical VaR by the 0.55%. At the 99% confidence level, the best model is WIP, which overestimates the empirical VaR by the 2.10%. In the TVaR case, one can see that regardless of the considered confidence level, the best model is the WIP, which indicates that our proposed models do not perform better than the competing models. Figure 6 shows grid maps of all model results with BIC vs. the results of VaR and TVaR. The grid map is proposed by [Blostein and Miljkovic \(2019\)](#) as a tool for model selection by using the entire space of models under consideration. Here again, the proposed seven models have the more conservative

Table 3: Danish fire insurance claims: model selection measures

Model	Npars	NLL	AIC	Ranking	BIC	Ranking
ComGBII	7	3814.22	7642.44	4	7683.19	11
GBIIG	6	3813.89	7639.79	2	7674.71	8
BIIG	5	3849.71	7709.41	12	7738.52	13
BG	5	3813.94	7637.88	1	7666.98	1
IBG	5	3817.91	7645.81	8	7674.92	10
PG	4	3818.06	7644.12	6	7667.40	2
IPG	4	3851.67	7711.34	13	7734.62	12
WIW	4	3820.01	7648.02	9	7671.30	3
PIW	4	3820.14	7648.28	10	7671.56	4
IBW	5	3816.34	7642.68	5	7671.79	5
WIP	4	3820.93	7649.87	11	7673.15	6
IBIP	5	3817.07	7644.14	7	7673.25	7
IBB	6	3814.00	7639.99	3	7674.92	9

* WIW, PIW, IBW, WIP, IBP, IBB represent Weibull-Inverse Weibull, Paralogistic-Inverse Weibull, Inverse Burr-Inverse Weibull, Weibull-Inverse Paralogistic, Inverse Burr-Inverse Paralogistic and Inverse Burr-Burr composite distribution proposed in [Grün and Miljkovic \(2019\)](#). The six models are selected as the 6 best fitting composite models (according to the BIC) when estimated to the Danish fire loss data.

* Npars denotes the number of estimated parameters.

* Best performance is in boldface.

 Table 4: Danish fire insurance claims: correlation R of QQ-plots, and KS, AD and CvM goodness-of-fit tests.

Model	R	Kolmogorov-Smirnov		Anderson-Darling		Cramer-von Mises	
		Statistics	P-value	Statistics	P-value	Statistics	P-value
ComGBII	0.999	0.013	0.966	$+\infty$	0.000	0.065	0.905
GBIIG	0.998	0.014	0.909	0.628	0.906	0.074	0.861
GIIG	0.996	0.020	0.682	1.514	0.671	0.127	0.792
BG	0.998	0.014	0.921	0.725	0.846	0.081	0.841
IBG	0.998	0.014	0.937	0.619	0.892	0.073	0.848
PG	0.998	0.014	0.908	0.727	0.843	0.081	0.849
IPG	0.996	0.023	0.580	1.766	0.658	0.159	0.752
WIW	-	0.021	0.222	1.159	0.284	-	-
PIW	-	0.021	0.226	1.156	0.285	-	-
IBW	-	0.021	0.216	1.160	0.283	-	-
WIP	-	0.021	0.210	1.318	0.227	-	-
IBIP	-	0.021	0.211	1.327	0.224	-	-
IBB	-	0.015	0.636	0.711	0.550	-	-

* The bootstrap p-values are computed using parametric bootstrap with 2000 simulation runs.

* The results of competing models are obtained in [Grün and Miljkovic \(2019\)](#). The correlation R of QQ-plots and Cramer-von Mises are not reported in their study.

Table 5: Danish fire insurance claims: summary of the results for VaR and TVaR at the 0.95 and 0.99 confidence level, obtained for the composite GBII models and previously fitted composited models.

Model	VaR				TVaR			
	0.95	Diff.%	0.99	Diff..%	0.95	Diff.%	0.99	Diff.%
Empirical	8.41	-	24.61	-	22.16	-	54.60	-
ComGBII	8.26	-1.77	25.60	4.02	27.81	25.52	86.22	57.91
GBIIG	8.23	-2.10	25.32	2.86	27.27	23.10	83.91	53.67
BIIG	8.33	-0.87	26.15	6.26	28.80	30.01	90.41	65.57
BG	8.28	-1.48	25.74	4.59	28.04	26.57	87.16	59.63
IBG	8.25	-1.90	25.46	3.42	27.52	24.22	84.95	55.58
PG	8.28	-1.48	25.74	4.58	28.04	26.56	87.15	59.61
IPG	8.36	-0.55	26.36	7.11	29.19	31.76	92.06	68.59
WIW	8.02	-4.60	22.77	-7.49	22.64	2.19	63.86	16.95
PIW	8.02	-4.60	22.79	-7.41	22.67	2.32	64.00	17.21
IBW	8.01	-4.71	22.73	-7.65	22.59	1.96	63.67	16.60
WIP	8.03	-4.48	22.64	-8.02	22.38	1.02	62.65	14.74
IBIP	8.03	-4.48	22.65	-7.98	22.39	1.06	62.69	14.81
IBB	8.22	-2.22	25.13	2.10	26.88	21.33	82.15	50.45

risk measures while they all show smaller BIC values than the competing models.

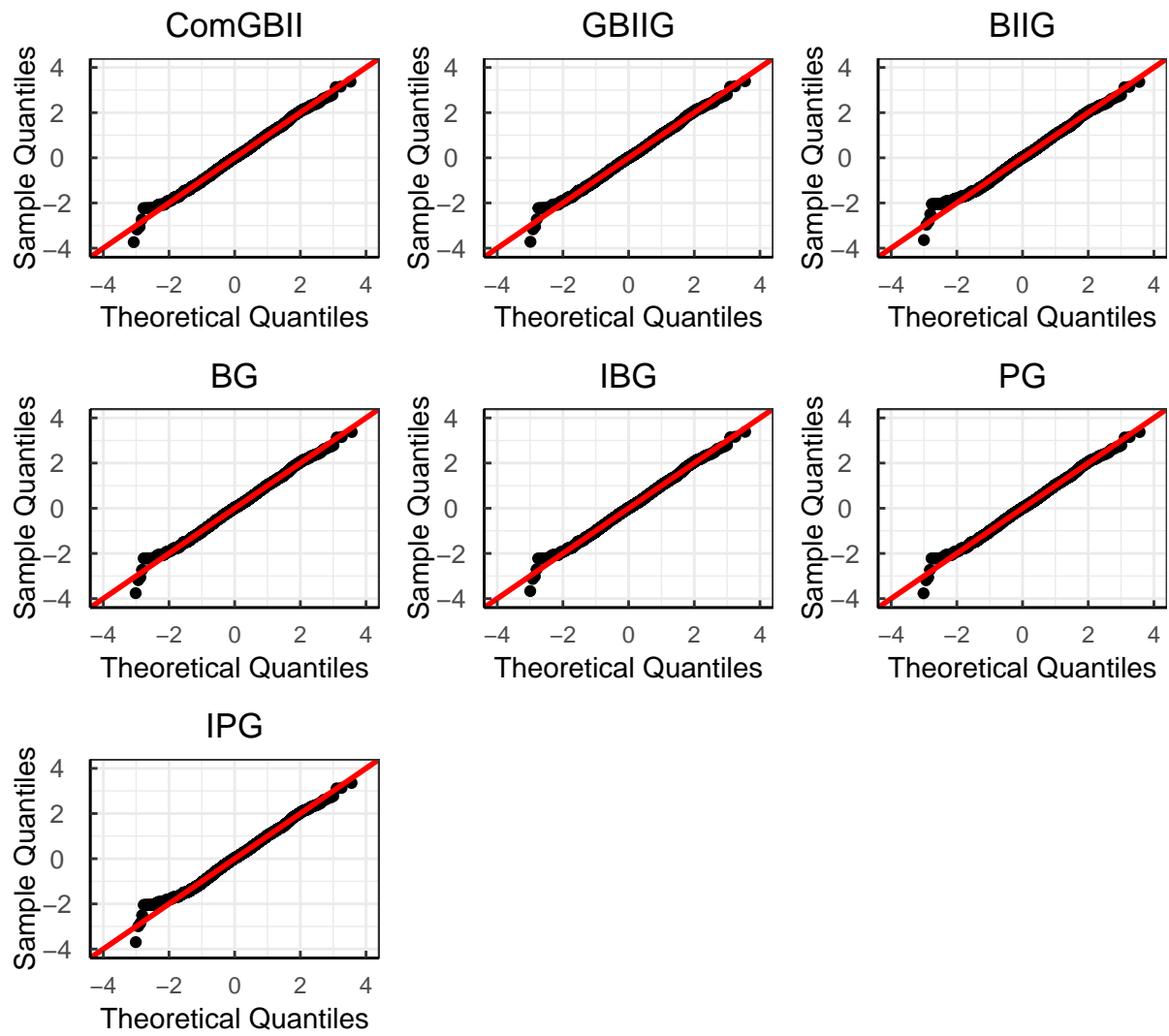


Figure 5: Danish fire insurance claims: QQ-plots of the empirical quantiles against the estimated model quantiles.

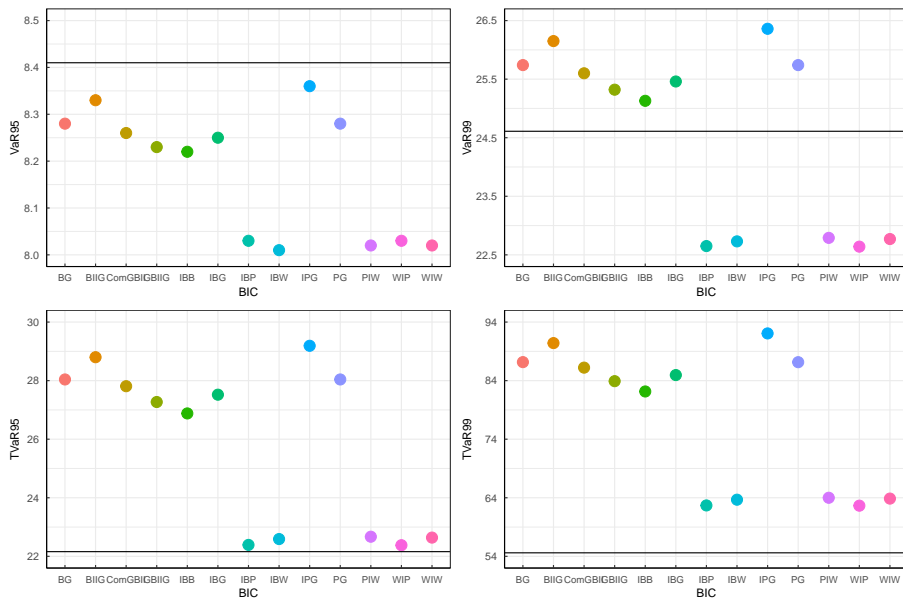


Figure 6: Top row shows grid maps of all model results with BIC vs. VaR_{0.95} (left) and VaR_{0.99} (right). Bottom row shows grid maps of all model results with BIC vs. TVaR_{0.95} (left) and TVaR_{0.99} (right). The empirical VaR and TVaR are shown as the horizontal line. The x-axis is ordered by BIC values, e.g., BG model has the smallest BIC, followed by BIIG while WIW has the largest BIC value.

5.2 Medical insurance data set

As the second example, we consider a medical insurance data set that was kindly provided by a major insurance company operating in China and concerns a short-term medical insurance that covers individual inpatient claim data. The data contains 19,110 policies between 2014 and 2016. Each claim records the positive inpatient claim amount, and several covariates, including *Gender*, *Age*, *SSCoverage*, *HospitalDays* and *ClaimType*. The summary statistics of these variables are shown in Table 6 and the histogram, the empirical density and the log-log plot of claim amounts are given in Figure 7. The empirical density is unimodal and highly skewed. The log-log plot seems asymptotically linear for the largest 10% of the claim amounts which indicates the tail is heavy-tailed. Figure 8 shows how the covariates from Table 6 are distributed in the medical insurance data-set. More than half of the policyholders (51.41%) have the social medical insurance or public medical insurance coverage, and more than half of the policyholders (55.63%) are female. Most policyholders (87.45%) have applied for insurance claims for MTD, 10.45% for MTA and only 2.10% for other level which includes the disability from disease (DSD), death from disease (DED), disability from accident (DSA), death from accident (DEA) and major disease (MD). Almost all policyholders (93.73%) are aged between 25 and 60, which means that there are few young and old inpatients in the insurance portfolio. Most of the policyholders in the insurance portfolio have been hospitalized less than 30 days (97.93%).

Table 6: Medical insurance claim data set: description of variables.

Variables	Type	Description
Claim amount	Continuous	inpatient (positive) claim amount of a patient ¥3-200,000
Age	Continuous	inpatient's age: 18-67
Gender	Categorical	male, female
SSCoverage	Categorical	social medical insurance or public medical insurance coverage: 0-1
HospitalDays	Continuous	the duration of hospitalization of a inpatient: 0-184 days
		reasons for claiming the medical insurance claim:
ClaimType	Categorical	medical treatment from disease (MTD), medical treatment from accident (MTA), other

For our analysis, we split the data set $\mathcal{L}(Y_i, \mathbf{x}_i)_{0 \leq i \leq n}$ into a training set \mathcal{U} that is used for model fitting, and a testing set \mathcal{V} which we (only) use for an out-of-sample analysis in proportion 60:40. We fit the distribution of claim amounts by incorporating covariates through the ComGBII regression and its

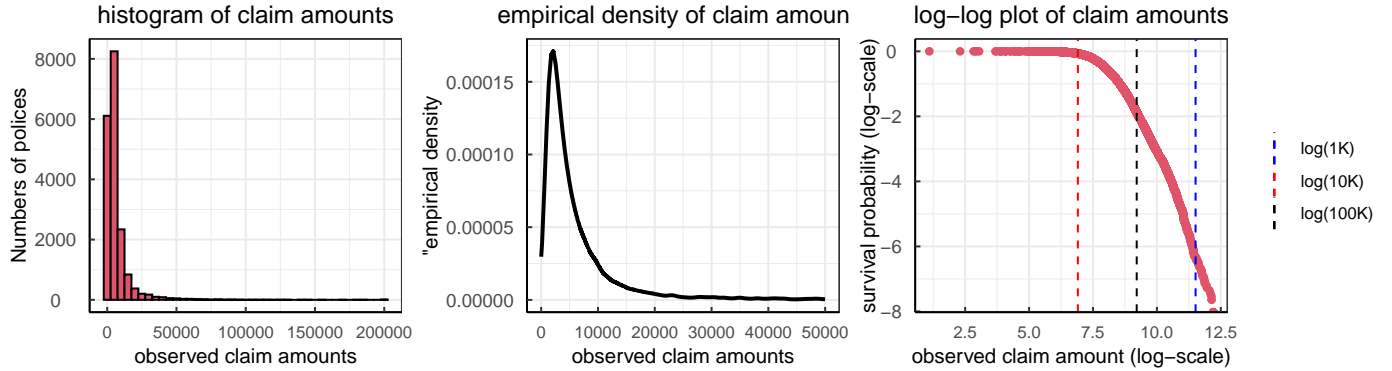


Figure 7: *Left panel:* histogram of the (positive) claim amounts of individual polices; *Middle panel:* empirical density (upper-truncated at 50,000); *Right panel:* log-log plot of observed claim amounts.

subfamilies discussed above (GBIIG, BIIG, BG, IBG, PG, IPG), illustrating how the covariates have significant effect on the claim amount paid for each insurance policy. The results are also compared with the GBII regression model ([Shi and Yang, 2018](#)), the generalized log-Moyal regression model (GlogM) discussed in [Bhati and Ravi \(2018\)](#), the the Burr regression discussed in [Beirlant et al. \(1998\)](#), and two log-link GLMs (Gamma regression and inverse Gaussian regression). Specifically, the covariates are introduced in modelling the location parameter in GBII by using the log link. The NLL, AIC and BIC values of the different fitted models are reported in Table 7. The fitted ComGBII regression model is the best regarding the AIC followed by the GBII, IBG and GBIIG regressions. The GBII model is the best regarding the BIC criterion followed by the PG, IBG and ComGBII regressions. Overall, the proposed seven regression models have a better performance than GLMs and other two heavy-tailed regression models, e.g., Burr and GlogM. To demonstrate the goodness of fit of the proposed models, we also provide in Figure 9 the QQ-plots of the quantile residuals $r_i = \Phi^{-1}[F(y_i; \hat{\gamma})]$ for the competing models, where $\hat{\gamma}$ denotes the estimates of parameters. It clearly indicates a preference for the ComGBII and GBII regression models that provide a considerably good fit for estimating the entire distribution of claim amounts in general. The upper tails of distribution can be better fitted by applying the ComGBII model than GBII model. The conventional GLMs and Burr regressions do not have advantages of capturing both small and large amounts of the claim data.

The results of the fitted ComGBII using all the covariates are reported in Table 8, along with GBII regression and two GLMs. The standard errors, Z-statistics and P-values are obtained from a normal approximation using the implied Fisher matrix based on the observed Hessian matrix from the numerical optimization, as detailed in Section 3. One can see that most of levels on the covariates are

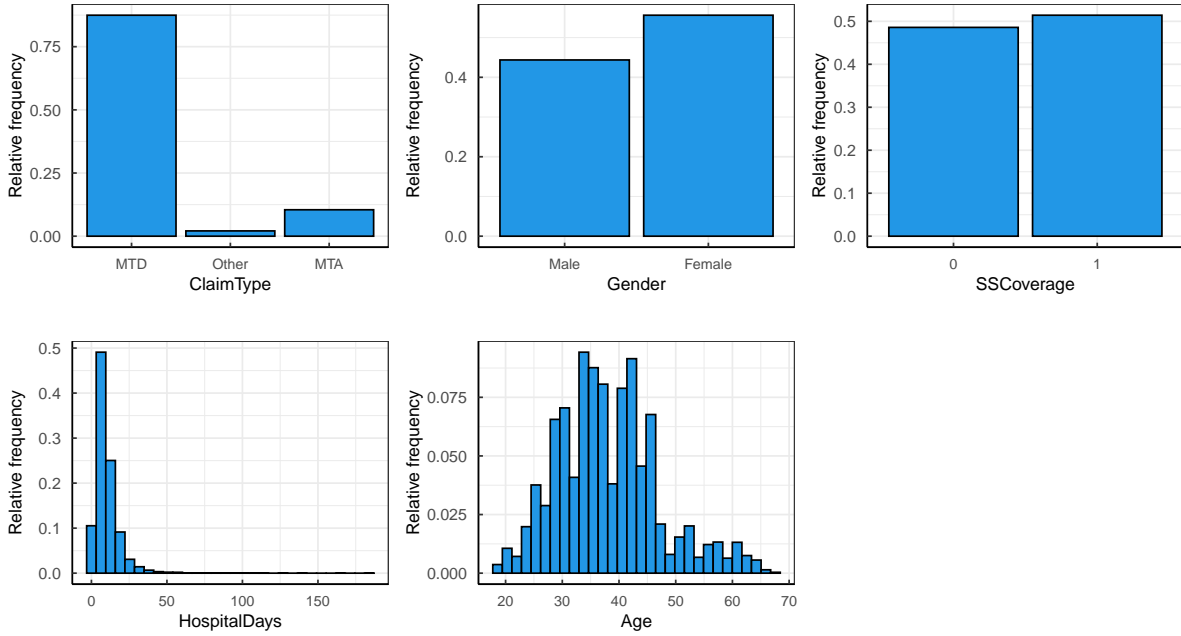


Figure 8: Relative frequency of the covariates *Gender*, *Age*, *SSCoverage*, *HospitalDays* and *ClaimType*.

Table 7: Medical insurance claim data set (in-sample): model selection.

Models	Npars	NLL	AIC	Ranking	BIC	Ranking
ComGBII	17	107601.9	215229.8	1	215325.1	4
GBIIG	16	107610.9	215245.7	4	215333.7	5
BIIG	15	107624.6	215271.2	8	215351.8	8
BG	15	107619.8	215261.6	6	215342.2	7
IBG	15	107610.7	215243.5	3	215324.1	3
PG	14	107615.3	215250.5	5	215323.8	2
IPG	14	107622.7	215265.4	7	215338.7	6
Burr	13	108917.6	217853.3	11	217919.2	11
GlogM	12	110664.7	221345.4	12	221404.1	12
GBII	14	107609.2	215238.3	2	215311.6	1
GA	12	108618.4	217252.8	10	217311.4	10
IG	12	108500.5	217017.0	9	217075.7	9

* GA and IG represent the Gamma and inverse Gaussian regression models.

* Best performance is in boldface.

highly significant (i.e. p-values less than 0.05) in ComGBII model except MTA level on *ClaimType*, which indicate these levels are important in explaining both the body and tail of claim distribution. Comparing effects of all the covariates for the four models, we notice that the nature of effect for a variable differs based on the model. For instance, MTA and other level on *ClaimType* shows significant

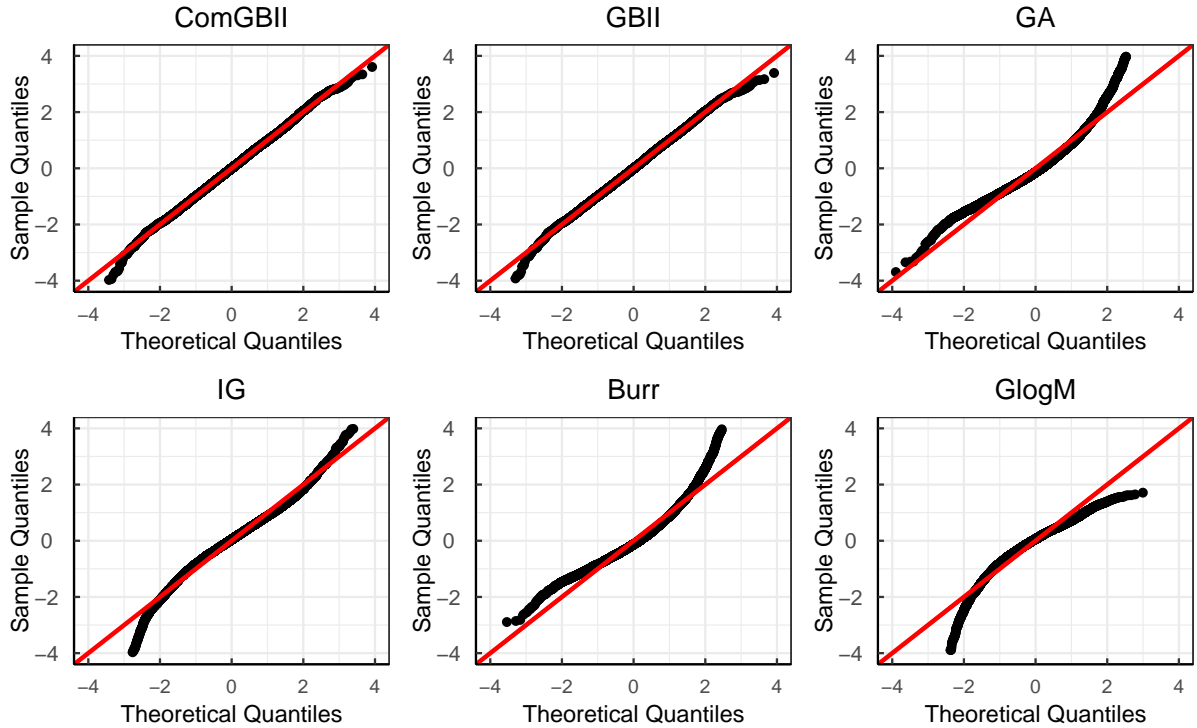


Figure 9: Training data set: normal QQ-plots of quantile residuals r_i from ComGBII regression model, together with the three heavy tailed regression model as well as two GLMs.

positive effects for the two GLMs, while they are significantly negative in the ComGBII and GBII models. *Gender* and *SSCoverage*, *Age* and *HospitalDays* have the same effects for the four models. Note that the estimated $\hat{p}_1\hat{\tau}_1 > 1$ and $\hat{p}_2\hat{\tau}_2 > 1$ in the ComGBII regression indicates the (theoretical) mean does not exist for all individual claims. The VaR measures of ComGBII model can be used for prediction, which are proportional to some exponential transformation of the linear combinations of covariates. It gives an intuitive interpretation for the insurance classification ratemaking and reserving when modelling more extreme claim data. For instance, the estimate results in ComGBII model reveal that the estimated VaR of inpatients in female group are $\exp(-0.03) = 0.970$ times more than male group.

In order to investigating the in-sample and out-of-sample performance of the proposed ComGBII regression, Figure 10 shows empirical (red dots) vs. fitted (green dots) log-log plots of claim amounts for randomly selected four risk classes on the training data and testing data respectively. The estimated threshold $\hat{u}(\mathbf{x}_i)$ in the fitted ComGBII distribution is marked as a blue vertical line. The values of threshold across all individuals are between 1,085 (minimum) and 2,774,989 (maximum), which

Table 8: Medical insurance claim data set: estimation results of ComGBII regression model and two GLMs .

Parameters	ComGBII				GBII			
	Estimates	S.E.	Z-statistics	P-value	Estimates	S.E.	Z-statistics	P-value
Intercept	5.35	0.14	39.27	0.00	7.80	0.05	155.78	0.00
Gender_Female	-0.03	0.02	-1.94	0.05	-0.03	0.02	-1.94	0.05
Age	0.00	0.00	4.58	0.00	0.00	0.00	4.58	0.00
ClaimType_Other	0.98	0.06	15.35	0.00	1.00	0.06	16.92	0.00
ClaimType_MTA	-0.02	0.03	-0.66	0.51	-0.03	0.03	-1.01	0.31
SSCoverage_1	-0.37	0.02	-21.14	0.00	-0.37	0.02	-22.50	0.00
HospitalDays	0.04	0.00	34.27	0.00	0.04	0.00	36.01	0.00
$\log(p_1)$	1.31	0.32	4.09	0.00	0.49	0.06	7.72	0.00
$\log(p_2)$	-0.38	0.05	-8.07	0.00	0.36	0.10	3.66	0.00
$\log(\tau_1)$	-4.73	8.25	-0.57	0.57	0.27	0.10	2.69	0.01
$\log(\tau_2)$	1.43	0.09	15.44	0.00	0.00	0.00	0.00	0.00
$\log(\nu_1)$	-0.56	0.35	-1.61	0.11	0.00	0.00	0.00	0.00
$\log(\nu_2)$	3.12	0.08	38.45	0.00	0.00	0.00	0.00	0.00
Parameters	GLMs-GA				GLMs-IG			
	Estimates	S.E.	Z-statistics	P-value	Estimates	S.E.	Z-statistics	P-value
Intercept	8.09	0.04	220.22	0.00	8.04	0.05	167.40	0.00
Gender_Female	-0.03	0.02	-1.92	0.05	-0.02	0.02	-0.79	0.43
Age	0.01	0.00	7.49	0.00	0.00	0.00	4.05	0.00
ClaimType_Other	1.00	0.06	17.94	0.00	1.03	0.13	7.68	0.00
ClaimType_MTA	0.18	0.03	6.63	0.00	0.13	0.04	3.36	0.00
SSCoverage_1	-0.33	0.02	-20.02	0.00	-0.31	0.02	-14.55	0.00
HospitalDays	0.05	0.00	40.64	0.00	0.06	0.00	25.07	0.00
$\log(\phi)$	-0.16	0.01	-26.09	0.00	-4.18	0.01	-627.63	0.00

* The estimates of dispersion parameter ϕ in GA regression and IG regression are $\exp(-0.16)$ and $\exp(-4.18)$ respectively.

indicates that the proposed model gives a good model fit for the tail part above the varying threshold related to different observed risk features. It also reflects the policyholder heterogeneity among the upper tail part of claim amounts.

Table 9 compares the in-sample and out-of-sample forecast performance of the different models investigated on the predicted $\hat{Y}_{i,q} = \text{VaR}_q(Y_i; \mathbf{x}_i)$ for individual risk features \mathbf{x}_i over the six quantile level q with the rang $[0.2, 0.8]$ ². We evaluate the mean squared error (MSE) for the competing models

²We use the estimated VaR measures over different quantile levels for prediction instead of estimated mean as the theoretical mean does not exist for all individuals in the medical insurance data set.

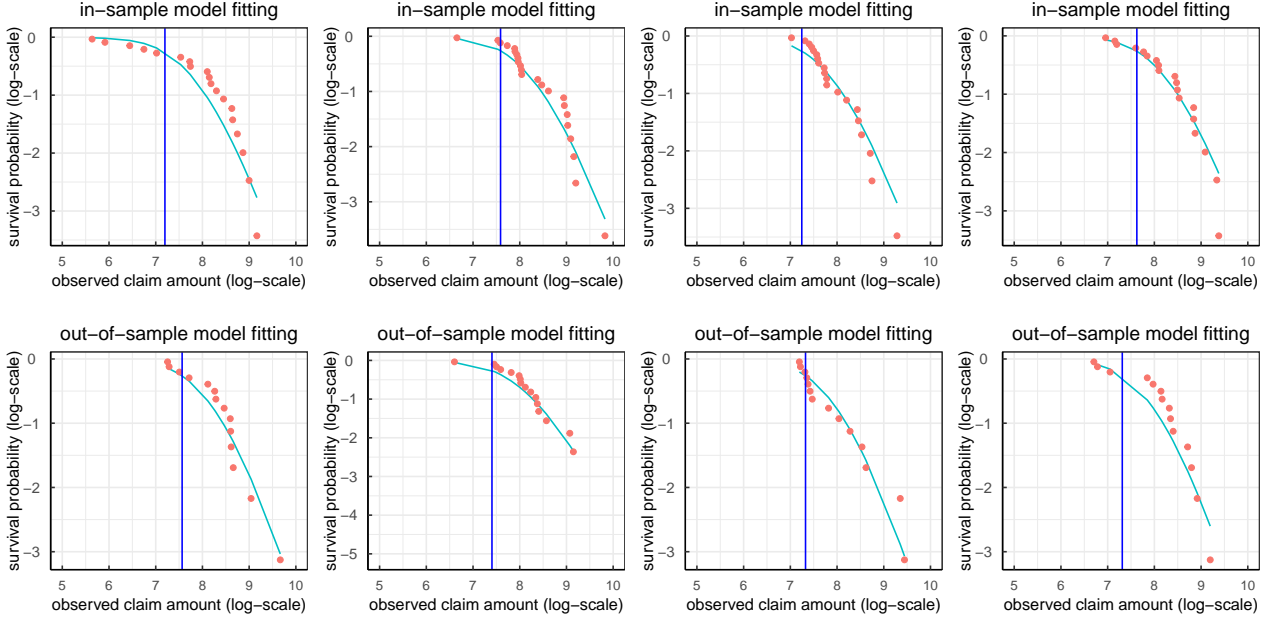


Figure 10: empirical (red dots) vs. fitted (green dots) log-log plots of claim amounts for randomly selected four risk classes on the training data (*Top*) and testing data (*Bottom*). The estimated threshold $\hat{u}(\mathbf{x}_i)$ based on the risk features in the fitted ComGBII distribution is marked as a blue vertical line.

see (5.1) and (5.2) respectively, on the training data and testing data.

$$\text{MSE}_q^{\text{in-sample}} = \sum_{(y_i, \mathbf{x}_i) \in \mathcal{U}} [y_i - \hat{Y}_{i,q}]^2, \quad (5.1)$$

$$\text{MSE}_q^{\text{out-of-sample}} = \sum_{(y_i, \mathbf{x}_i) \in \mathcal{V}} [y_i - \hat{Y}_{i,q}]^2. \quad (5.2)$$

We note that ComGBII and BIIG regression models show a better in-sample model performance than other seven models. A clear ranking of the out-of-sample MSEs at different quantile levels among the different models is also observed. The BIIG regression as a subfamily of the proposed models is most predictive, consistently leading to the lowest MSEs. Next in line is ComGBII and the GLMs with Gamma distributed assumption is the least predictive for claim amounts. Figure 11 shows the estimated $\text{VaR}_q(Y_i; \mathbf{x}_i)$ at quantile level $q : 10\%; 50\%; 90\%$ (blue, black, blue) on the training data \mathcal{U} and test data \mathcal{V} for the BIIG model. The individual sample observations are ordered w.r.t. the estimated median in black. It can be observed that this order monotonicity for all quantiles. The red dots show the corresponding observed claim amount, most of which fall in the interval between the

estimated $\text{VaR}_q(Y_i; \mathbf{x}_i)$ at $q = 10\%$ and $q = 90\%$.

Table 9: In-sample and out-of-sample MSE_p , $p \in [0.2, 0.8]$, on the training data \mathcal{U} and testing data \mathcal{V} of nine regression models.

Models/ q	out-of-sample MSE_q					in-sample MSE_q				
	20%	40%	50%	60%	80%	20%	40%	50%	60%	80%
ComGBII	3.17	6.19	8.81	12.92	34.80	8.06	19.63	29.47	44.85	125.83
GBIIG	3.41	7.03	10.10	14.77	38.14	9.13	23.27	35.08	52.92	141.57
BIIG	3.08	6.20	8.79	12.70	32.25	7.93	20.21	30.26	45.29	119.77
BG	3.17	6.45	9.18	13.29	33.84	8.30	21.23	31.82	47.67	126.13
IBG	3.39	6.99	10.04	14.68	37.88	9.08	23.17	34.94	52.69	140.85
PG	3.21	6.54	9.33	13.55	34.63	8.44	21.54	32.35	48.56	128.95
IPG	3.12	6.32	8.97	12.97	32.97	8.11	20.70	31.00	46.40	122.67
GBII	3.15	6.25	8.87	12.90	33.71	8.10	20.17	30.18	45.51	123.80
GA	16.61	59.51	97.62	154.86	402.15	62.92	237.07	391.54	623.33	1623.97

* The results are reported are scaled by 10^{-8} .

* The smallest MSE is in bold.

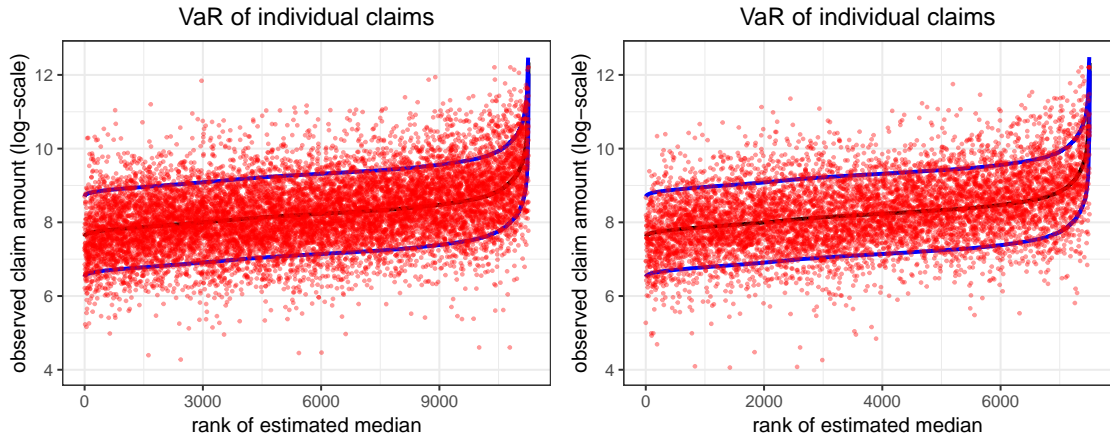


Figure 11: Estimated $\text{VaR}_q(Y_i; \mathbf{x}_i)$ of BIIG regression model at quantile level $q : 10\%; 50\%; 90\%$ (blue, black, blue) on the training data \mathcal{U} (*Left panel*) and test data \mathcal{V} (*Right panel*). The red dots show the corresponding sample observations (realizations) Y_i ; the x-axis orders the claims w.r.t. the estimated median $\text{VaR}_{50\%}(Y_i; \mathbf{x}_i)$ (in black).

6 Conclusion

In this paper, we have proposed a versatile composite distribution based on the GBII family allowing closed-form expressions for a lot of insurance measures and have studied some of its properties. This new model is design to model the entire range of loss data which is achieved by splicing two GBII distributions as the head and the tail respectively based on mode-matching method. It also contains a wide range of insurance loss distributions provides the close-formed expressions for statistical modelling and estimation. Finally, the proposed model is found more appropriate as compared to several other composite models as discussed in existing literature using the well-known Danish insurance loss data-set.

Another interesting contribution of this paper is that the regression modelling is discussed in the composite GBII distribution for presenting high flexibility since covariates can be introduced in the location parameter in a non-linear form, being therefore an alternative to the heavy tailed regression model. It not only provides a suitable fit for the entire range of data apart from the body, but capture the risk heterogeneity by allowing the varying threshold across individuals that are related to risk features. Moreover, it can be also used as an important complement to the conventional GLMs in the non-life insurance classification ratemaking mechanism for modelling extreme losses data when the mean does not exist.

It is worth mentioning that the composite regression models we considered in this work were parametric, and it would be semiparametric or approach when functional forms other than the linear are included in the location parameters of the models. Another extension of this work could be devoted to the regularization approach, boosting or neural network algorithm in the regression setting that allows us to investigate more complex effects of the covariates on the insurance losses.

Acknowledgement

Zhengxiao Li acknowledges the financial support from National Natural Science Fund of China (Grant No. 71901064), the University of International Business and Economics project for Outstanding Young Scholars (Grant No. 20YQ16), and “the Fundamental Research Funds for the Central Universities” in UIBE (Grant No. CXTD13-02).

Appendices

A The gradients of the log-likelihood function

The first order partial derivatives of the log-likelihood function $\partial\ell(\boldsymbol{\beta}, \boldsymbol{\alpha}; \mathbf{y})$, with respect to $\boldsymbol{\alpha} = (\alpha_1, \dots, \alpha_6)$ can be calculated based on the following equations:

$$\begin{aligned}\frac{\partial\ell(\boldsymbol{\beta}, \boldsymbol{\alpha}; \mathbf{y})}{\partial p_1} &= I[y_i \leq u(\mathbf{x}_i; \boldsymbol{\beta})] \sum_{i=1}^n \frac{1}{r(\boldsymbol{\alpha})} \frac{\partial r(\boldsymbol{\alpha})}{\partial p_1} \\ &\quad + I[y_i \leq u(\mathbf{x}_i; \boldsymbol{\beta})] \sum_{i=1}^n \frac{1}{f_{\text{GBII}}(y_i; \mu_1(\mathbf{x}_i; \boldsymbol{\beta}), p_1, \nu_1, \tau_1)} \frac{\partial f_{\text{GBII}}(y_i; \mu_1(\mathbf{x}_i; \boldsymbol{\beta}), p_1, \nu_1, \tau_1)}{\partial p_1} \\ &\quad - I[y_i \leq u(\mathbf{x}_i; \boldsymbol{\beta})] \sum_{i=1}^n \frac{1}{I_{\nu_1, \tau_1} \left[\frac{p_1 \nu_1 - 1}{p_1 \nu_1 + p_1 \tau_1} \right]} \frac{\partial I_{\nu_1, \tau_1} \left[\frac{p_1 \nu_1 - 1}{p_1 \nu_1 + p_1 \tau_1} \right]}{\partial p_1} \\ &\quad + I[y_i > u(\mathbf{x}_i; \boldsymbol{\beta})] \sum_{i=1}^n \frac{1}{r(\boldsymbol{\alpha}) - 1} \frac{\partial r(\boldsymbol{\alpha})}{\partial p_1},\end{aligned}$$

$$\begin{aligned}\frac{\partial\ell(\boldsymbol{\beta}, \boldsymbol{\alpha}; \mathbf{y})}{\partial p_2} &= I[y_i \leq u(\mathbf{x}_i; \boldsymbol{\beta})] \sum_{i=1}^n \frac{1}{r(\boldsymbol{\alpha})} \frac{\partial r(\boldsymbol{\alpha})}{\partial p_2} \\ &\quad + I[y_i > u(\mathbf{x}_i; \boldsymbol{\beta})] \sum_{i=1}^n \frac{1}{r(\boldsymbol{\alpha}) - 1} \frac{\partial r(\boldsymbol{\alpha})}{\partial p_2} \\ &\quad + I[y_i > u(\mathbf{x}_i; \boldsymbol{\beta})] \sum_{i=1}^n \frac{1}{f_{\text{GBII}}(y_i; \mu_2(\mathbf{x}_i; \boldsymbol{\beta}), p_2, \nu_2, \tau_2)} \frac{\partial f_{\text{GBII}}(y_i; \mu_2(\mathbf{x}_i; \boldsymbol{\beta}), p_2, \nu_2, \tau_2)}{\partial p_2} \\ &\quad + I[y_i > u(\mathbf{x}_i; \boldsymbol{\beta})] \sum_{i=1}^n \frac{1}{1 - I_{\nu_2, \tau_2} \left[\frac{p_2 \nu_2 - 1}{p_2 \nu_2 + p_2 \tau_2} \right]} \frac{\partial I_{\nu_2, \tau_2} \left[\frac{p_2 \nu_2 - 1}{p_2 \nu_2 + p_2 \tau_2} \right]}{\partial p_2},\end{aligned}$$

$$\begin{aligned}
\frac{\partial \ell(\boldsymbol{\beta}, \boldsymbol{\alpha}; \mathbf{y})}{\partial \tau_1} &= I[y_i \leq u(\mathbf{x}_i; \boldsymbol{\beta})] \sum_{i=1}^n \frac{1}{r(\boldsymbol{\alpha})} \frac{\partial r(\boldsymbol{\alpha})}{\partial \tau_1} \\
&+ I[y_i \leq u(\mathbf{x}_i; \boldsymbol{\beta})] \sum_{i=1}^n \frac{1}{f_{\text{GBII}}(y_i; \mu_1(\mathbf{x}_i; \boldsymbol{\beta}), p_1, \nu_1, \tau_1)} \frac{\partial f_{\text{GBII}}(y_i; \mu_1(\mathbf{x}_i; \boldsymbol{\beta}), p_1, \nu_1, \tau_1)}{\partial \tau_1} \\
&- I[y_i \leq u(\mathbf{x}_i; \boldsymbol{\beta})] \sum_{i=1}^n \frac{1}{I_{\nu_1, \tau_1} \left[\frac{p_1 \nu_1 - 1}{p_1 \nu_1 + p_1 \tau_1} \right]} \frac{\partial I_{\nu_1, \tau_1} \left[\frac{p_1 \nu_1 - 1}{p_1 \nu_1 + p_1 \tau_1} \right]}{\partial \tau_1} \\
&+ I[y_i > u(\mathbf{x}_i; \boldsymbol{\beta})] \sum_{i=1}^n \frac{1}{r(\boldsymbol{\alpha}) - 1} \frac{\partial r(\boldsymbol{\alpha})}{\partial \tau_1},
\end{aligned}$$

$$\begin{aligned}
\frac{\partial \ell(\boldsymbol{\beta}, \boldsymbol{\alpha}; \mathbf{y})}{\partial \tau_2} &= I[y_i \leq u(\mathbf{x}_i; \boldsymbol{\beta})] \sum_{i=1}^n \frac{1}{r(\boldsymbol{\alpha})} \frac{\partial r(\boldsymbol{\alpha})}{\partial \tau_2} \\
&+ I[y_i > u(\mathbf{x}_i; \boldsymbol{\beta})] \sum_{i=1}^n \frac{1}{r(\boldsymbol{\alpha}) - 1} \frac{\partial r(\boldsymbol{\alpha})}{\partial \tau_2} \\
&+ I[y_i > u(\mathbf{x}_i; \boldsymbol{\beta})] \sum_{i=1}^n \frac{1}{f_{\text{GBII}}(y_i; \mu_2(\mathbf{x}_i; \boldsymbol{\beta}), p_2, \nu_2, \tau_2)} \frac{\partial f_{\text{GBII}}(y_i; \mu_2(\mathbf{x}_i; \boldsymbol{\beta}), p_2, \nu_2, \tau_2)}{\partial \tau_2} \\
&+ I[y_i > u(\mathbf{x}_i; \boldsymbol{\beta})] \sum_{i=1}^n \frac{1}{1 - I_{\nu_2, \tau_2} \left[\frac{p_2 \nu_2 - 1}{p_2 \nu_2 + p_2 \tau_2} \right]} \frac{\partial I_{\nu_2, \tau_2} \left[\frac{p_2 \nu_2 - 1}{p_2 \nu_2 + p_2 \tau_2} \right]}{\partial \tau_2},
\end{aligned}$$

$$\begin{aligned}
\frac{\partial \ell(\boldsymbol{\beta}, \boldsymbol{\alpha}; \mathbf{y})}{\partial \nu_1} &= I[y_i \leq u(\mathbf{x}_i; \boldsymbol{\beta})] \sum_{i=1}^n \frac{1}{r(\boldsymbol{\alpha})} \frac{\partial r(\boldsymbol{\alpha})}{\partial \nu_1} \\
&+ I[y_i \leq u(\mathbf{x}_i; \boldsymbol{\beta})] \sum_{i=1}^n \frac{1}{f_{\text{GBII}}(y_i; \mu_1(\mathbf{x}_i; \boldsymbol{\beta}), p_1, \nu_1, \tau_1)} \frac{\partial f_{\text{GBII}}(y_i; \mu_1(\mathbf{x}_i; \boldsymbol{\beta}), p_1, \nu_1, \tau_1)}{\partial \nu_1} \\
&- I[y_i \leq u(\mathbf{x}_i; \boldsymbol{\beta})] \sum_{i=1}^n \frac{1}{I_{\nu_1, \tau_1} \left[\frac{p_1 \nu_1 - 1}{p_1 \nu_1 + p_1 \tau_1} \right]} \frac{\partial I_{\nu_1, \tau_1} \left[\frac{p_1 \nu_1 - 1}{p_1 \nu_1 + p_1 \tau_1} \right]}{\partial \nu_1} \\
&+ I[y_i > u(\mathbf{x}_i; \boldsymbol{\beta})] \sum_{i=1}^n \frac{1}{r(\boldsymbol{\alpha}) - 1} \frac{\partial r(\boldsymbol{\alpha})}{\partial \nu_1},
\end{aligned}$$

$$\begin{aligned}
\frac{\partial \ell(\boldsymbol{\beta}, \boldsymbol{\alpha}; \mathbf{y})}{\partial \nu_2} &= I[y_i \leq u(\mathbf{x}_i; \boldsymbol{\beta})] \sum_{i=1}^n \frac{1}{r(\boldsymbol{\alpha})} \frac{\partial r(\boldsymbol{\alpha})}{\partial \nu_2} \\
&\quad + I[y_i > u(\mathbf{x}_i; \boldsymbol{\beta})] \sum_{i=1}^n \frac{1}{r(\boldsymbol{\alpha}) - 1} \frac{\partial r(\boldsymbol{\alpha})}{\partial \nu_2} \\
&\quad + I[y_i > u(\mathbf{x}_i; \boldsymbol{\beta})] \sum_{i=1}^n \frac{1}{f_{\text{GBII}}(y_i; \mu_2(\mathbf{x}_i; \boldsymbol{\beta}), p_2, \nu_2, \tau_2)} \frac{\partial f_{\text{GBII}}(y_i; \mu_2(\mathbf{x}_i; \boldsymbol{\beta}), p_2, \nu_2, \tau_2)}{\partial \nu_2} \\
&\quad + I[y_i > u(\mathbf{x}_i; \boldsymbol{\beta})] \sum_{i=1}^n \frac{1}{1 - I_{\nu_2, \tau_2} \left[\frac{p_2 \nu_2 - 1}{p_2 \nu_2 + p_2 \tau_2} \right]} \frac{\partial I_{\nu_2, \tau_2} \left[\frac{p_2 \nu_2 - 1}{p_2 \nu_2 + p_2 \tau_2} \right]}{\partial \nu_2}.
\end{aligned}$$

Note that the gradients of the $r(\boldsymbol{\alpha})$, $f_{\text{GBII}}(y_i; \mu_j(\mathbf{x}_i; \boldsymbol{\beta}), p_j, \nu_j, \tau_j)$ and $I_{\nu_j, \tau_j} \left[\frac{p_j \nu_j - 1}{p_j \nu_j + p_j \tau_j} \right]$ for $j = 1, 2$ can be calculated based on the following equations. For simplicity, the subscripts of $I_{\nu_j, \tau_j}(\pi_j)$ and $f_{\text{GBII}}(y_i; \mu_j(\mathbf{x}_i; \boldsymbol{\beta}), p_j, \nu_j, \tau_j)$ are omitted. First, the partial derivatives of $r(\boldsymbol{\alpha})$ are given by:

$$\begin{aligned}
\frac{\partial r(\boldsymbol{\alpha})}{\partial p_1} &= \frac{\frac{\partial I_{\nu_1, \tau_1}(\pi_1)}{\partial p_1} \omega - I_{\nu_1, \tau_1}(\pi_1) \left[\frac{\partial I_{\nu_1, \tau_1}(\pi_1)}{\partial p_1} + \frac{\partial \phi}{\partial p_1} (1 - I_{\nu_2, \tau_2}(\pi_2)) \right]}{\omega^2}, \\
\frac{\partial r(\boldsymbol{\alpha})}{\partial p_2} &= \frac{-I_{\nu_1, \tau_1}(\pi_1) \left[\frac{\partial \phi}{\partial p_2} [1 - I_{\nu_2, \tau_2}(\pi_2)] - \phi \frac{\partial I_{\nu_2, \tau_2}(\pi_2)}{\partial p_2} \right]}{\omega^2}, \\
\frac{\partial r(\boldsymbol{\alpha})}{\partial \tau_1} &= \frac{\frac{\partial I_{\nu_1, \tau_1}(\pi_1)}{\partial \tau_1} \omega - I_{\nu_1, \tau_1}(\pi_1) \left[\frac{\partial I_{\nu_1, \tau_1}(\pi_1)}{\partial \tau_1} + \frac{\partial \phi}{\partial \tau_1} (1 - I_{\nu_2, \tau_2}(\pi_2)) \right]}{\omega^2}, \\
\frac{\partial r(\boldsymbol{\alpha})}{\partial \tau_2} &= \frac{-I_{\nu_1, \tau_1}(\pi_1) \left[\frac{\partial \phi}{\partial \tau_2} [1 - I_{\nu_2, \tau_2}(\pi_2)] - \phi \frac{\partial I_{\nu_2, \tau_2}(\pi_2)}{\partial \tau_2} \right]}{\omega^2}, \\
\frac{\partial r(\boldsymbol{\alpha})}{\partial \nu_1} &= \frac{\frac{\partial I_{\nu_1, \tau_1}(\pi_1)}{\partial \nu_1} \omega - I_{\nu_1, \tau_1}(\pi_1) \left[\frac{\partial I_{\nu_1, \tau_1}(\pi_1)}{\partial \nu_1} + \frac{\partial \phi}{\partial \nu_1} (1 - I_{\nu_2, \tau_2}(\pi_2)) \right]}{\omega^2}, \\
\frac{\partial r(\boldsymbol{\alpha})}{\partial \nu_2} &= \frac{-I_{\nu_1, \tau_1}(\pi_1) \left[\frac{\partial \phi}{\partial \nu_2} [1 - I_{\nu_2, \tau_2}(\pi_2)] - \phi \frac{\partial I_{\nu_2, \tau_2}(\pi_2)}{\partial \nu_2} \right]}{\omega^2},
\end{aligned}$$

where

$$\begin{aligned}
\omega &= I_{\nu_1, \tau_1} \left[\frac{p_1 \nu_1 - 1}{p_1 \nu_1 + p_1 \tau_1} \right] + \phi \left\{ 1 - I_{\nu_2, \tau_2} \left[\frac{p_2 \nu_2 - 1}{p_2 \nu_2 + p_2 \tau_2} \right] \right\}, \\
\pi_1 &= \frac{p_1 \nu_1 - 1}{p_1 \nu_1 + p_1 \tau_1}, \\
\pi_2 &= \frac{p_2 \nu_2 - 1}{p_2 \nu_2 + p_2 \tau_2}, \\
\frac{\partial \phi}{\partial p_1} &= \phi \left[\frac{1}{p_1} + \frac{\nu_1 + \tau_1}{p_1(p_1 \nu_1 - 1)(p_1 \tau_1 + 1)} \right], \\
\frac{\partial \phi}{\partial p_2} &= -\phi \left[\frac{1}{p_2} + \frac{\nu_2 + \tau_2}{p_2(p_2 \nu_2 - 1)(p_2 \tau_2 + 1)} \right], \\
\frac{\partial \phi}{\partial \tau_1} &= \phi \left[\ln \frac{p_1 \tau_1 + 1}{p_1 \nu_1 + p_1 \tau_1} - \frac{1}{p_1 \tau_1 + 1} - \psi(\tau_1) + \psi(\nu_1 + \tau_1) \right], \\
\frac{\partial \phi}{\partial \tau_2} &= \phi \left[\ln \frac{p_2 \nu_2 + p_2 \tau_2}{p_2 \tau_2 + 1} + \frac{1}{p_2 \tau_2 + 1} + \psi(\tau_2) - \psi(\nu_2 + \tau_2) \right], \\
\frac{\partial \phi}{\partial \nu_1} &= \phi \left[\ln \frac{p_1 \nu_1 - 1}{p_1 \nu_1 + p_1 \tau_1} + \frac{1}{p_1 \nu_1 - 1} - \psi(\nu_1) + \psi(\nu_1 + \tau_1) \right], \\
\frac{\partial \phi}{\partial \nu_2} &= \phi \left[\ln \frac{p_2 \nu_2 + p_2 \tau_2}{p_2 \nu_2 - 1} - \frac{1}{p_2 \nu_2 - 1} + \psi(\nu_2) - \psi(\nu_2 + \tau_2) \right],
\end{aligned}$$

with $\psi(\cdot)$ denotes the Digamma function.

Then, we need to calculate the partial derivatives of $I_{\nu, \tau}(\pi) = I_{\nu, \tau} \left[\frac{p\nu - 1}{p\nu + p\tau} \right]$ which are given by

$$\begin{aligned}
\frac{\partial I_{\nu, \tau}(\pi)}{\partial p} &= \frac{\partial I_{\nu, \tau} \left[\frac{p\nu - 1}{p\nu + p\tau} \right]}{\partial p} = \frac{(p\tau + 1)^{(\tau-1)}(p\nu - 1)^{(\nu-1)}}{B(\nu, \tau)p(p\nu + p\tau)^{(\nu+\tau-1)}}, \\
\frac{\partial I_{\nu, \tau}(\pi)}{\partial \tau} &= \frac{\partial I_{\nu, \tau} \left[\frac{p\nu - 1}{p\nu + p\tau} \right]}{\partial \tau} = \frac{\Gamma(\tau)\Gamma(\nu + \tau)}{\Gamma(\nu)} \left[(1 - \pi)^\tau {}_3F_2(\tau, \tau, 1 - \nu; \tau + 1, \tau + 1; 1 - \pi) \right] \\
&\quad + I_{\tau, \nu}(1 - \pi) [\psi(\tau) - \psi(\nu + \tau) - \log(1 - \pi)], \\
\frac{\partial I_{\nu, \tau}(\pi)}{\partial \nu} &= \frac{\partial I_{\nu, \tau} \left[\frac{p\nu - 1}{p\nu + p\tau} \right]}{\partial \nu} = -\frac{\Gamma(\nu)\Gamma(\nu + \tau)}{\Gamma(\tau)} \left[\pi^\nu {}_3F_2(\nu, \nu, 1 - \tau; \nu + 1, \nu + 1; \pi) \right] \\
&\quad + I_{\nu, \tau}(\pi) [\psi(\nu + \tau) - \psi(\nu) + \log(\pi)],
\end{aligned}$$

where ${}_3F_2(\cdot)$ denotes the Regularized generalized hypergeometric function, with *alist* contain three-parameters and *blist* contain two parameters.

Finally, the partial derivatives of $f_{\text{GBII}}(y_i; \mu(\mathbf{x}_i; \boldsymbol{\beta}), p, \nu, \tau)$ with respected to p , τ and ν are given

by

$$\begin{aligned}\frac{\partial f_{\text{GBII}}(y_i; \mu(\mathbf{x}_i; \boldsymbol{\beta}), p, \nu, \tau)}{\partial p} &= f_{\text{GBII}}(y_i; \mu(\mathbf{x}_i; \boldsymbol{\beta}), p, \nu, \tau) \left[\frac{1}{p} + \frac{\tau y_i^p \ln \frac{\mu(\mathbf{x}_i; \boldsymbol{\beta})}{y_i} + \nu \mu(\mathbf{x}_i; \boldsymbol{\beta})^p \ln \frac{y_i}{\mu(\mathbf{x}_i; \boldsymbol{\beta})}}{y_i^p + \mu(\mathbf{x}_i; \boldsymbol{\beta})^p} \right], \\ \frac{\partial f_{\text{GBII}}(y_i; \mu(\mathbf{x}_i; \boldsymbol{\beta}), p, \nu, \tau)}{\partial \tau} &= f_{\text{GBII}}(y_i; \mu(\mathbf{x}_i; \boldsymbol{\beta}), p, \nu, \tau) \left[\ln \frac{\mu(\mathbf{x}_i; \boldsymbol{\beta})^p}{y_i^p + \mu(\mathbf{x}_i; \boldsymbol{\beta})^p} \right], \\ \frac{\partial f_{\text{GBII}}(y_i; \mu(\mathbf{x}_i; \boldsymbol{\beta}), p, \nu, \tau)}{\partial \nu} &= f_{\text{GBII}}(y_i; \mu(\mathbf{x}_i; \boldsymbol{\beta}), p, \nu, \tau) \left[\ln \frac{y_i^p}{y_i^p + \mu(\mathbf{x}_i; \boldsymbol{\beta})^p} \right].\end{aligned}$$

The first order partial derivatives of the log-likelihood function $\partial \ell(\boldsymbol{\beta}, \boldsymbol{\alpha}; \mathbf{y})$, with respect to $\boldsymbol{\beta}$ are give by:

$$\begin{aligned}\frac{\partial \ell(\boldsymbol{\beta}, \boldsymbol{\alpha}; \mathbf{y})}{\partial \boldsymbol{\beta}} &= I[y_i \leq u(\mathbf{x}_i; \boldsymbol{\beta})] \sum_{i=1}^n \frac{1}{f_{\text{GBII}}(y_i; \mu_1(\mathbf{x}_i; \boldsymbol{\beta}), p_1, \nu_1, \tau_1)} \frac{\partial f_{\text{GBII}}(y_i; \mu_1(\mathbf{x}_i; \boldsymbol{\beta}), p_1, \nu_1, \tau_1)}{\partial \mu_1(\mathbf{x}_i; \boldsymbol{\beta})} \frac{\partial \mu_1(\mathbf{x}_i; \boldsymbol{\beta})}{\partial \boldsymbol{\beta}} \\ &\quad + I[y_i > u(\mathbf{x}_i; \boldsymbol{\beta})] \sum_{i=1}^n \frac{1}{f_{\text{GBII}}(y_i; \mu_2(\mathbf{x}_i; \boldsymbol{\beta}), p_2, \nu_2, \tau_2)} \frac{\partial f_{\text{GBII}}(y_i; \mu_2(\mathbf{x}_i; \boldsymbol{\beta}), p_2, \nu_2, \tau_2)}{\partial \mu_2(\mathbf{x}_i; \boldsymbol{\beta})} \frac{\partial \mu_2(\mathbf{x}_i; \boldsymbol{\beta})}{\partial \boldsymbol{\beta}},\end{aligned}$$

where

$$\begin{aligned}\frac{\partial f_{\text{GBII}}(y_i; \mu(\mathbf{x}_i; \boldsymbol{\beta}), p, \nu, \tau)}{\partial \boldsymbol{\beta}} &= \frac{\partial f_{\text{GBII}}(y_i; \mu(\mathbf{x}_i; \boldsymbol{\beta}), p, \nu, \tau)}{\partial \mu(\mathbf{x}_i; \boldsymbol{\beta})} \frac{\partial \mu(\mathbf{x}_i; \boldsymbol{\beta})}{\partial \boldsymbol{\beta}} \\ &= f_{\text{GBII}}(y_i; \mu(\mathbf{x}_i; \boldsymbol{\beta}), p, \nu, \tau) \frac{p [\tau y_i^p - \nu \mu(\mathbf{x}_i; \boldsymbol{\beta})^p]}{\mu(\mathbf{x}_i; \boldsymbol{\beta}) [y_i^p + \mu(\mathbf{x}_i; \boldsymbol{\beta})^p]} \frac{\partial \mu(\mathbf{x}_i; \boldsymbol{\beta})}{\partial \boldsymbol{\beta}}.\end{aligned}$$

B Distribution nested within the GBII distribution

Table 10: Distribution nested within the GBII distribution

Distribution	Npar	Density function	
GBII	4	GBII(p, μ, ν, τ)	$\frac{ p }{B(\nu, \tau)y} \frac{\mu^{p\tau} y^{p\nu}}{(y^p + \mu^p)^{\nu+\tau}}$
Beta distribution of the second kind	3	BII(μ, ν, τ)	GBII(1, μ, ν, τ)
Burr	3	B(p, μ, τ)	GBII($p, \mu, 1, \tau$)
Inverse Burr	3	IB(p, ν, τ)	GBII($p, \mu, \nu, 1$)
GLMGA	3	G(p, μ, ν)	GBII($p, \mu, \nu, \frac{1}{2}$)
Inverse GLMGA	3	IG(p, μ, τ)	GBII($p, \mu, \frac{1}{2}, \tau$)
Paralogistic	2	PL(p, μ)	GBII($p, \mu, 1, p$)
Inverse Paralogistic	2	IPL(p, μ)	GBII($p, \mu, p, 1$)

References

- Adelchi Azzalini, Thomas Del Cappello, Samuel Kotz, et al. Log-skew-normal and log-skew-t distributions as models for family income data. *Journal of Income Distribution*, 11(3):12–20, 2002.
- SA Abu Bakar, NA Hamzah, M Maghsoudi, and S Nadarajah. Modeling loss data using composite models. *Insurance: Mathematics and Economics*, 61:146–154, 2015.
- Jan Beirlant, Yuri Goegebeur, Robert Verlaak, and Petra Vynckier. Burr regression and portfolio segmentation. *Insurance: Mathematics and Economics*, 23(3):231–250, 1998.
- Mauro Bernardi, Antonello Maruotti, and Lea Petrella. Skew mixture models for loss distributions: a bayesian approach. *Insurance: Mathematics and Economics*, 51(3):617–623, 2012.
- Deepesh Bhati and Sreenivasan Ravi. On generalized log-moyal distribution: A new heavy tailed size distribution. *Insurance: Mathematics and Economics*, 79:247–259, 2018.

Martin Bladt. Phase-type distributions for claim severity regression modeling. *ASTIN Bulletin: The Journal of the IAA*, pages 1–32, 2022.

Martin Blostein and Tatjana Miljkovic. On modeling left-truncated loss data using mixtures of distributions. *Insurance: Mathematics and Economics*, 85:35–46, 2019.

Enrique Calderín-Ojeda and Chun Fung Kwok. Modeling claims data with composite stoppa models. *Scandinavian Actuarial Journal*, 2016(9):817–836, 2016.

JSK Chan, STB Choy, UE Makov, and Z Landsman. Modelling insurance losses using contaminated generalised beta type-II distribution. *ASTIN Bulletin: The Journal of the IAA*, 48(2):871–904, 2018.

Kahadawala Cooray and Malwane MA Ananda. Modeling actuarial data with a composite lognormal-pareto model. *Scandinavian Actuarial Journal*, 2005(5):321–334, 2005.

J David Cummins, Georges Dionne, James B McDonald, and B Michael Pritchett. Applications of the gb2 family of distributions in modeling insurance loss processes. *Insurance: Mathematics and Economics*, 9(4):257–272, 1990.

Joan del Castillo, Jalila Daoudi, and Isabel Serra. The full tails gamma distribution applied to model extreme values. *ASTIN Bulletin: The Journal of the IAA*, 47(3):895–917, 2017.

Alice XD Dong and JSK Chan. Bayesian analysis of loss reserving using dynamic models with generalized beta distribution. *Insurance: Mathematics and Economics*, 53(2):355–365, 2013.

Peter K Dunn and Gordon K Smyth. Randomized quantile residuals. *Journal of Computational and Graphical Statistics*, 5(3):236–244, 1996.

Tobias Fissler, Michael Merz, and Mario V Wüthrich. Deep quantile and deep composite model regression. *arXiv preprint arXiv:2112.03075*, 2021.

Tsz Chai Fung, George Tzougas, and Mario Wuthrich. Mixture composite regression models with multi-type feature selection. *arXiv preprint arXiv:2103.07200*, 2021.

Guojun Gan and Emiliano A Valdez. Fat-tailed regression modeling with spliced distributions. *North American Actuarial Journal*, 22(4):554–573, 2018.

Philip E Gill, Walter Murray, and Michael A Saunders. Snopt: An sqp algorithm for large-scale constrained optimization. *SIAM review*, 47(1):99–131, 2005.

Emilio Gómez-Déniz, Enrique Calderín-Ojeda, and José María Sarabia. Gamma-generalized inverse gaussian class of distributions with applications. *Communications in Statistics-Theory and Methods*, 42(6):919–933, 2013.

Bettina Grün and Tatjana Miljkovic. Extending composite loss models using a general framework of advanced computational tools. *Scandinavian Actuarial Journal*, 2019(8):642–660, 2019.

Stuart A Klugman, Harry H Panjer, and Gordon E Willmot. *Loss models: from data to decisions*, volume 715. John Wiley & Sons, 2012.

Zinoviy Landsman, Udi Makov, and Tomer Shushi. Tail conditional moments for elliptical and log-elliptical distributions. *Insurance: Mathematics and Economics*, 71:179–188, 2016.

Christian Laudagé, Sascha Desmettre, and Jörg Wenzel. Severity modeling of extreme insurance claims for tariffication. *Insurance: Mathematics and Economics*, 88:77–92, 2019.

Zhengxiao Li, Jan Beirlant, and Shengwang Meng. Generalizing the log-moyal distribution and regression models for heavy-tailed loss data. *ASTIN Bulletin: The Journal of the IAA*, 51(1):57–99, 2021.

Tatjana Miljkovic and Bettina Grün. Modeling loss data using mixtures of distributions. *Insurance: Mathematics and Economics*, 70:387–396, 2016.

S. Nadarajah and S. A. A. Bakar. New composite models for the danish fire insurance data. *Scandinavian Actuarial Journal*, 2014(2):180–187, 2014.

Jorge Nocedal and Stephen Wright. *Numerical optimization*. Springer Science & Business Media, 2006.

Antonio Punzo, Luca Bagnato, and Antonello Maruotti. Compound unimodal distributions for insurance losses. *Insurance: Mathematics and Economics*, 81:95–107, 2018.

Tom Reynkens, Roel Verbelen, Jan Beirlant, and Katrien Antonio. Modelling censored losses using splicing: A global fit strategy with mixed erlang and extreme value distributions. *Insurance: Mathematics and Economics*, 77:65–77, 2017.

David PM Scollnik. On composite lognormal-pareto models. *Scandinavian Actuarial Journal*, 2007 (1):20–33, 2007.

David PM Scollnik and Chenchen Sun. Modeling with weibull-pareto models. *North American Actuarial Journal*, 16(2):260–272, 2012.

Peng Shi and Lu Yang. Pair copula constructions for insurance experience rating. *Journal of the American Statistical Association*, 113(521):122–133, 2018.

George Tzougas and Dimitris Karlis. An em algorithm for fitting a new class of mixed exponential regression models with varying dispersion. *ASTIN Bulletin: The Journal of the IAA*, 50(2):555–583, 2020.

Roel Verbelen, Lan Gong, Katrien Antonio, Andrei Badescu, and Sheldon Lin. Fitting mixtures of erlangs to censored and truncated data using the em algorithm. *ASTIN Bulletin: The Journal of the IAA*, 45(3):729–758, 2015.

Yinyu Ye. *Interior algorithms for linear, quadratic, and linearly constrained non-linear programming*. PhD thesis, Ph. D. thesis, Department of ESS, Stanford University, 1987.